Addis Ababa University

Addis Ababa Institute of Technology

School of Electrical and Computer Engineering

CONTROL OF GRID CONNECTED MICRO HYDRO POWER SYSTEM

A Thesis Submitted to the School of Graduate Studies, Addis Ababa Institute of Technology in Partial Fulfillment of the Requirements for the Degree of Master of Science in Electrical and Computer Engineering (Control Engineering)

By

Getachew Nadew

Advisor: Dr. Mengesha Mamo

January, 2020

Addis Ababa University
Addis Ababa Institute of Technology
School of Electrical and Computer Engineering

CONTROL OF GRID CONNECTED MICRO HYDRO POWER SYSTEM

By

Getachew Nadew

Approved by Board of Examiners

_____	_____
Chairman, Department of Graduate Committee	Signature
Dr. Mengesha Mamo	_____
Advisor	Signature
_____	_____
Internal Examiner	Signature
_____	_____
External Examiner	Signature

DECLARATION

I, the undersigned declare that this thesis is my original work, and has not been presented for a degree in this or any other university, and all sources of materials used for the thesis have been fully acknowledged.

Getachew Nadew

_____

Name

Signature

Addis Ababa, Ethiopia

January, 2020

Place

Date of submission

This thesis has been submitted with my approval as a university advisor

Dr. Mengesha Mamo

_____

Advisor Name

Signature

ACKNOWLEDGMENTS

First of all, I would like to give glory to ALMIGHTY GOD without his help, the completion of this thesis would have been unimaginable. Next, I would like to express my deepest gratitude to my advisor, *Dr. Mengesha Mamo* for his expert guidance, constructive comments, suggestions and encouragement.

Last but not least, I would like to thank my friends and my colleague in Control Engineering students for their patience, encouragement and love.

Table of Contents

ACKNOWLEDGMENTS iii
LIST OF TABLES vi
LIST OF SYMBOLS ix
LIST OF ABBREVIATIONS xi
ABSTRACT xii
CHAPTER ONE: INTRODUCTION 1
1.2 Background 1
1.2 Problem Statement 2
1.3 Objectives of the thesis 3
1.3.1. General objective: 3
1.3.2. Specific objectives: 3
1.4 Methodology 4
1.5 Thesis outline 6
CHAPTER TWO: LITERATURE REVIEW 7
2.1 Introduction 7
2.2 Micro-Hydro Power Plant 7
2.3 Micro Hydro Power Development 8
2.3.1 Electro Mechanical Components 9
2.4 Pulse Width Modulation 12
2.5 Phase locked loop for grid synchronization 13
2.5.1 Stationary reference frame αβ 15
2.5.2 Synchronous rotating reference frame based PLL 15
2.6 Previous Works on Grid Connected of Micro Hydropower Plant 17
CHAPTER THREE: MICRO HYDRO POWER TURBINE AND PERMANENT MAGNET SYNCHRONOUS GENERATOR MODELING 19
3.1 Modeling of micro hydro power turbine 19
3.1.1 A simplified model of the hydro turbine. 20
3.1.2 Linear Turbine modeling 22
3.2 Modeling of permanent magnet synchronous generator 25
3.2.1 Introduction of PMSG 25

3.2.2 Mathematical model of PMSG in natural ABC frame 26
3.2.3 Mathematical model of PMSG in rotational d-q frame 27
3.2.4. Electrical torque and power analysis 29
CHAPTER FOUR: MHP CONVERTERS AND CONTROL COMPONENT DESIGN 31
4.1 AC to DC Rectifier 31
4.2 Boost converter 35
4.3 Grid tie Inverter Design 40
4.3.1 The three phase voltage source inverter 41
4.3.2 LC Filter 41
4.4 PLL design 44
CHAPTER FIVE: SIMULATION RESULTS AND DISCUSSIONS 49
5.1 Introduction 49
5.2 Simulation Results 49
5.2.1 Simulation for ideal grid conditions 49
5.2.2 Simulation for non-ideal grid conditions 51
5.3 Discussions 58
CHAPTER SIX: CONCLUSIONS, RECOMMENDATIONS AND FUTURE WORK 59
6.1 Conclusions 59
5.2 Recommendations and Future Work 60
REFERENCES 61
APPENDICES 64

LIST OF TABLES

Table 3. 1 Mean Monthly Flow Rate of Huluka River 21
Table 3. 2 Comparison of flow rates by their profit 21
Table 3. 3 Ethiopian Electric Utility tariffs..... 22
Table 4. 1 Performance parameters for three phase bridge rectifier..... 34
Table 4. 2 design parameters for LC filter..... 42

LIST OF FIGURES

Figure 1. 1 Flow chart of the research methodology of the thesis 5
Figure 2. 1 Micro hydropower plant overview with penstock [7]. 8
Figure 2. 2 Operation range of head and flow for different types of hydro power turbine [9]. 10
Figure 2. 3 The triangular carrier wave (red), sinusoidal reference wave (blue), and modulated and un modulated sine pulses [11]. 13
Figure 2. 4 Basic structure for the SRF PLL system 14
Figure 2. 5 Synchronous rotating reference frame [14] 16
Figure 2. 6 Simplified system for the SRF PLL. 17
Figure 3. 1 Insight view of Kaplan turbine operation principle with a generator [22]. 19
Figure 3. 2 The use of turbines with varying head [25] 23
Figure 3. 3 Design diagram for a Kaplan turbine [25] 23
Figure 3. 4 Cross view of three phase PMSG with a single pole pair [27] 26
Figure 3. 5 Equivalence circuit of PMSG in d-axis [10]. 28
Figure 3. 6 Equivalence circuit of PMSG in q-axis [10]. 28
Figure 3. 7 Serial-parallel testing circuit for the generator inductance [28] 29
Figure 4. 1 Three phase full bridge diode rectifier [30] 31
Figure 4. 2 Voltage and current waveforms of the three-phase bridge rectifier 32
Figure 4. 3 DC-DC boost converter topology with ideal switch and diode [29]. 35
Figure 4. 4 Circuit of boost converter when the ideal switch is on [31]. 35
Figure 4. 5 Circuit of boost converter when switch is off [31] 36
Figure 4. 6 Inductor voltage and capacitor current with a single switching cycle [31]. 37
Figure 4. 7 Ripple current on the inductor and ripple voltage on the capacitor in one duty cycle. 38
Figure 4. 8 DC boost converter output current and voltage wave form 40
Figure 4. 9 Three phase inverter [33]. 41
Figure 4. 10 LC filter 42
Figure 4. 11 α-β frame and rotational d-q frame decomposition with grid frequency ω and a random phase angle θ [13]. 43
Figure 4. 12 The Simulink Simulation Setup of the Phase Lock Loop System. The box named Discrete Transfer Fcn is the PI-regulator. 46

Figure 4. 13 a) Transformation from abc to α-β. Gain 5 is -$\sqrt{3}$/3 and gain 3 is $\sqrt{3}$/3. b) Transformation from α-β to dq. 46
Figure 4. 14 Over all block diagram implemented in simulink 48
Figure 5. 1 Output Waveforms of (a) Grid (b) inverter Voltages 50
Figure 5. 2 PLL output with ideal grid conditions. From the phase angle (yellow) a sine wave 50
Figure 5. 3 Output of PI-regulator, this can be thought of as a step response for the system. 51
Figure 5. 4 Vd output while the voltage space vector is synchronized with the q-axis. 51
Figure 5. 5 Input signals with amplitude decreasing to 90% of the original value 52
Figure 5. 6 PLL output for input with decreased amplitude 52
Figure 5. 7 PLL output for grid with frequency 55Hz. 53
Figure 5. 8 PI-regulator output of input signals with 55Hz frequency leads to a PI-regulator output of 31.4. 53
Figure 5. 9 PLL output for grid with frequency 45Hz. 53
Figure 5. 10 PI-regulator output of input signals with 45Hz frequency leads to a PI-regulator output of -31.4. 54
Figure 5. 11 Input Voltage with Phase Jump 54
Figure 5. 12 PLL Output for Input Signals with Phase Jump. 55
Figure 5. 13 Three-Phase Unbalanced Voltages Input. 55
Figure 5. 14 PLL Output for Input Signals with Unbalanced Voltages. 56
Figure 5. 15 PI-Regulator Output with Three Phase Voltage Unbalance Input Signal. 56
Figure 5. 16 PLL output for input signals with improper phase shifts 56
Figure 5. 17 The PI-regulator with input signals with improper phase shifts 57
Figure 5. 18 Active power that flows in to the grid 57
Figure 5. 19 Reactive power that flows in to the grid 57

LIST OF SYMBOLS

f	Frequency
p	Number of poles
rev	Revolutions
T_e	Electromagnetic torque
Q	Flow rate
g	Gravitational acceleration
η_t	Turbine efficiency
H	Hydraulic head
T_m	Mechanical torque
ωm	Mechanical rotation speed
P_t	Turbine output power
D	Duty cycle
ρ	Water density
N	Rotational speed of the turbine
N_s	Specific speed of the turbine
D_a	Inner diameter of the wheel
D_N	Outer diameter of the wheel
C_o	Relative velocity in meridian direction
u	Tangential velocity of the blade
Δw_u	Difference of the tangential velocity

w_{u1}	Tangential velocity at the leading edge
w_{u2}	Tangential velocity at the trailing edge
ω_e	Electrical rotation speed
λm	Flux linkage produced by the permanent magnet material
EMF	Electromotive force
η_r	Rectification ratio

LIST OF ABBREVIATIONS

AC	Alternating Current
CCM	Continuous Conduction Mode
CSI	Current Controlled Inverter
DC	Direct Current
DCM	Discontinuous Conduction Mode
EEPCo	Ethiopian Electric Power Corporation
FF	Form Factor
KW	Kilo Watt
LPF	Low Pass Filter
MHPP	Micro Hydro Power Plant
MHPT	Micro Hydro Power Turbine
MW	Mega Watt
PD	Phase Detector
PI	Proportional Integral
PLL	Phase Locked Loop
PWM	Pulse Width Modulation
SRF	Synchronously rotating Reference Frame
SVM	Space Vector Modulation
RF	Ripple Factor
VCI	Voltage Controlled Inverter
VCO	Voltage Controlled Oscillator
ZCD	Zero crossing detection

ABSTRACT

For a grid connected micro hydropower (MHP) system, power electronics and phase locked loop was designed and simulated in this research. The grid interconnection of MHP improve the reliability of the grid and helps to decrease transmission and distribution losses. However, the synchronization with the utility grid is the main concern of the inverter control design because the grid frequency, phase and voltage need to be tracked. If the inverter output cannot meet the local grid connection criteria, the power will not be allowed to deliver.

In this research, mathematical modeling of micro hydro power plant has been done. The full bridge three phase diode rectifier, boost converter, inverter and LC filter are designed to connect the power generated to the grid. Then, by injecting the grid voltage signal in to the PLL, the phase voltage frequency and phase angle has been tracked to synchronize phase, frequency and voltage of the generated power with different grid condition.

It is observed from the simulation results that for ideal grid conditions the phase angle was tracked and relatively faster and also precisely. Also the system can easily track the phase when the frequency was changed from 50Hz to 55Hz or 45Hz. The only difference from the ideal case is that the PI-regulator now approaches $2\pi*5$rad/s for 55 Hz and $-2\pi*5$rad/s for 45Hz instead of zero. Moreover, different non-ideal grid conditions were simulated and almost handled by the system.

Key words: Micro Hydropower, Power Converters, PI Regulator, Phase Locked Loop

CHAPTER ONE

INTRODUCTION

1.2 Background

Most of the developing countries are affliction from what many call the energy crisis, which is characterized by depletion of locally available energy resources and dependence on imported fuel. In fact, the energy crisis is supposed to be the second most serious problem in these countries next to the food crisis. What is more, it is exacerbating the food crisis by increasing the rate of deforestation and thereby causing degradation of farmlands. All these situations apply to Ethiopia. Traditional fuels contributed 99.9% of the rural area energy utilization, fuel wood contributes the most significant source (81.8%), next to fuel wood dung contributes (9.4%), crop residues (8.4%) and then the rest is contributed by charcoal [1].

However, MHPP was one of the earliest small scale renewable energy technologies to be developed, and is still an important source of energy today [2]. It has the potential to generate an important share of power more than solar and wind power with a low price. According to Ethiopian EEPCo classification of hydro power system, generation capacity of MHPP ranges from 11KW to 500KW and are thought to be ideal renewable resources to electrify isolated rural communities [3]. Due to the high potential of micro hydropower in Ethiopia, micro hydropower plants could play a positive role towards accelerating rural electrification process.

Common topologies of MHP are stand-alone operation used in rural areas in developing countries. However, smaller scale renewable energy becomes more access to the people in recent years due to the idea of the micro grid emerged. The micro grid is developed for localized electrical energy generation and distribution. Like other renewable resources in a micro grid, micro hydropower system can either deliver electric power to an isolated load or be connected to the grid [4].

On the other hand, in Ethiopia in the period between 1950 and 1970, EEPCo installed several MHP schemes with a total capacity of 1.5 MW. All of them are not operational anymore once the areas were connected to integrated connection system (ICS), the MHP plants were shut down.

In 2002 by the Irish Development Aid and the Sidama Development Program, 170 kW off-grid plant was commissioned; however, during the 2002/2003 dry season, it was suffered from low river flow. After only having operated for two years, EEPCo connected the area to ICS and the MHP plant was shut down completely. Moreover, the GIZ Energizing Development (EnDev) Ethiopia implemented four pilot MHP sites (cross-flow turbines) in the Sidama Zone (SNNPR) with a capacity of 7 kW (Gebecho I), 30 kW (Gebecho II), 33 kW (Ererte) and 55 kW (Hagara Sodicha) respectively and upgraded a watermill in Jimma Zone (Oromia Region) Leku into a 20 kW MHP, further a 10 kW MHP plant in Kersa. Additionally, it is conducting inclusive survey for the conversion of 30 traditional watermills into micro hydro-power schemes. The studies are undertaken jointly with established Centers of Excellence for Hydropower at inter alia Arba Minch & Jimma Universities [3].

At present, these MHPPs are faced the grid connection challenges. Most of these plants are running in an off-grid mode for local power supply. However, if the grid extended to those remote areas, many micro hydropower plants will be redundant if they can't be connected to the grid. Unless the grid connection requirement is met, many of the MHPP are forced to shut down [5].

1.2 Problem Statement

There are two ways of operation of micro-hydro: stand-alone mode and grid integration mode. Stand-alone mode is usually used in rural electrification to serve small load and applications where frequency regulation is not very critical. Despite the fact that, often off-grid MHPs operate at very low plant factor due to a lack of productive use of energy, resulting in sub-optimal exploitation of resources. In addition, if the grid extended to remote areas, many micro hydropower plant need to be redundant and they are forced to shut down unless the grid connection requirement is met.

However, grid interconnection of MHP generates additional revenue for the plant by increasing its plant factor and the total number of sold kWh’s from the mini-grid. If the feed-in tariff is higher than what the local consumers paid, then the benefit for the MHP is even higher. Both aspects can help to increase revenues and therefore, help to ensure long-term sustainability of the MHP. In addition, grid interconnection allows consumers in the local mini-grid to receive power from the utility when the MHP is not producing sufficient power to meet the local demand. In MHP villages wherever the

number of households and/or appliances has increased, or the water flow has decreased over time, deficiency of power is a common reality.

Furthermore, from the point of view of the national utility, the interconnection helps to reduce the consumption of fossil fuel, improves the reliability of the grid and also helps to decrease transmission and distribution losses. At present, these MHPPs face the grid connection challenges. Most of these plants are running in an off-grid mode for local power supply.

Here in this research power electronics (AC/DC, DC/DC and DC/AC) and Phase locked loop (PLL) are designed to integrate micro hydro power system with the distribution network at the interface with the grid. Power electronics as interface between PMSG and distribution system of the grid to improve the quality of power of the customer by reducing the harmonics created, providing reactive power control or voltage regulation at the distribution system connection point. In addition, the phase angle of the grid during its ideal and non ideal conditions were successfully tracked by using PLL.

1.3 Objectives of the thesis

1.3.1. General objective:

This research work is aimed at model, design and simulation of grid connected micro hydro power system control.

1.3.2. Specific objectives:

- Studying different grid connection mechanisms of micro hydropower systems.
- Modeling the micro hydro power turbine and the PMSG in natural ABC phase and rotational d-q axis.
- Designing the full bridge 3-Φ diode rectifier, boost converter, inverter based on pulse width modulator to connect the power generated to the grid and PLL to control the power flow (to track phase, frequency and voltage of the grid) and Power expression in synchronous d-q axis.
- Simulation of the synchronization of grid connected MHPP using MATLAB-Simulink.

1.4 Methodology

The following methodologies have been used for the accomplishment of this thesis:
First, the statement of the problem is described and the objectives of the research is defined. Next, different literatures of grid connection mechanisms of micro hydropower systems are studied. A comparison of previous similar research is also presented. This is followed by a detail mathematical modeling of MHPT and the permanent magnet synchronous generator in natural ABC phase and rotational d-q. The full bridge three phase diode rectifier, boost converter, inverter and LC filter are designed to connect the power generated to the grid. Then, phase lock loop is designed to synchronize the phase, frequency, and voltage of the generated power with different grid condition.

Simulation studies are carried out for ideal and non-ideal grid conditions. Finally conclusion is given based on the research findings. A flow chart representing the methodology of the thesis is shown in figure 1.1.

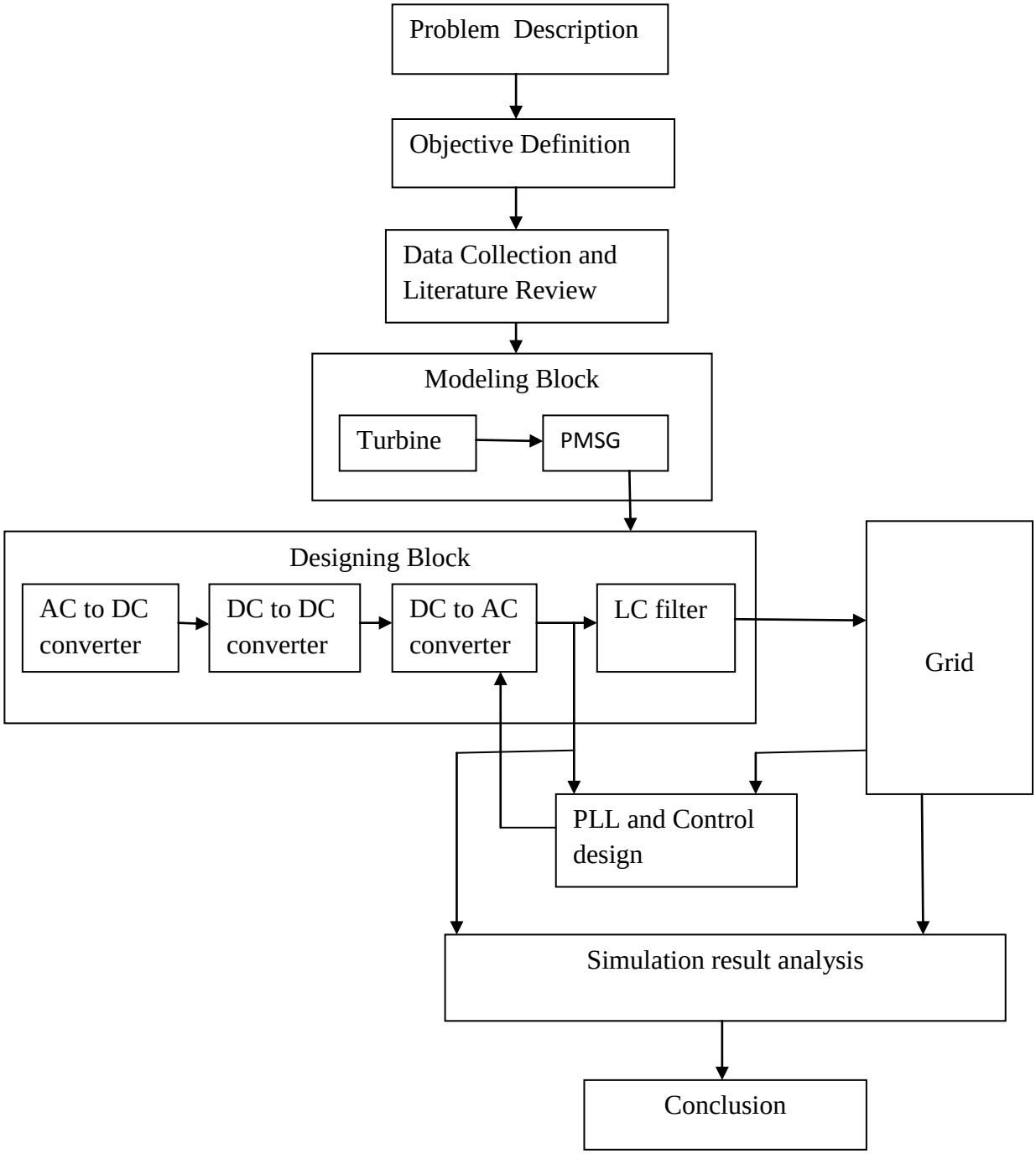

Figure 1. 1 Flow chart of the research methodology of the thesis

1.5 Thesis outline

The thesis is organized into six chapters. *Chapter one* presents the introduction, problem statement, objectives of the study and the methodology leading towards the completion of the thesis. *Chapter two* discusses about micro hydropower and its development, Pulse Width Modulation, Phase locked loop for grid synchronization. Finally, related works are discussed briefly. *Chapter three* deals with the detailed model of a micro hydropower plant. Modeling of MHPT and PMSG in natural ABC phase and rotational d-q axis are described in this chapter. A simplified model equation are also discussed in this chapter. *Chapter four* presents the full bridge three phase diode rectifier, boost converter and inverter to implement the AC to DC, DC to DC and DC to AC conversion design. The design of PLL is also presented in this chapter.

The grid connected MHPP simulation results obtained using MATLAB-Simulink and discussions of the results are presented in *chapter five*. *Chapter six* includes conclusions, recommendation and future work.

CHAPTER TWO

LITERATURE REVIEW

2.1 Introduction

In this chapter different grid connected micro hydropower systems, micro hydropower plant as well as development of micro hydropower are presented. In addition to this, the main components of MHPP, the components that are used to synchronize the MHPP to the grid are discussed in this chapter.

2.2 Micro Hydro Power Plant

A micro-hydropower system is a small system; according to Ethiopian EEPCo classification of hydro power system, generation capacity of micro hydropower plants ranges from 11KW to 500KW and are thought to be ideal renewable resources to electrify remote rural areas [3]. The micro hydropower concept is made for fully utilizing the renewable energy from the running water.

Traditional hydropower plants are usually constructed on large dams; however, micro hydro power systems are usually "flow of river" in which cut off the river is not required to build a dam for power generation. The flow of river system lets very short term water storage which provide more flexibility to handle different load situation. It is more economical than the traditional hydropower because flow of river methods cost much less than a reservoir dam. The other drawback of large hydropower plants from an environmental point of view is that ecosystem will be dramatically changed because of constructions of dams and hydropower plants. Even if the hydropower source is clean, it will damages the environment before the renewable energy is utilized. Also hydropower plants are not accessible for most people to construct because electricity generated by hydropower is targeted to be sent to the vast power network usually rated at 10 megawatts (MW) and a conventional hydropower plant normally associate with large dam construction.

However, in recent years, the idea of the micro grid provides people more access to smaller-scale renewable energy. The micro grid is developed for localized electricity generation and distribution.

Power sources and loads in a micro grid can be either grid connected or islanded [6]. Since the micro grid scheme is flexible distribution, hydropower can be sized to a smaller power rating for better utilization of the local reliable renewable resource. similar to other renewable resources in a micro grid, micro hydropower system can either deliver electric power to an isolated load or be connected to the integrated connection system [7].

2.3 Micro Hydro Power Development

A micro hydropower system consists of the following major parts:

1. water conveyance: storage sink, forebay or penstock.
2. micro-hydro turbine: converts energy of the flowing water in to mechanical energy.
3. generator and power control system: for energy conversion form mechanical to electrical energy and deliver the power to the local load or utility grid.

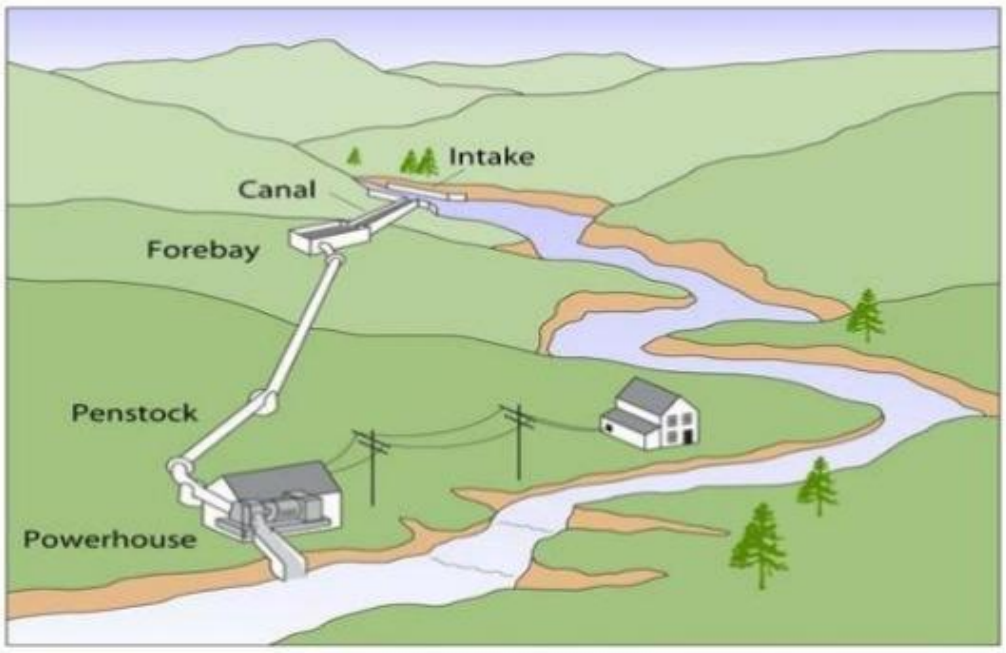

Figure 2. 1 Over all of micro hydropower plant with penstock [7].

Figure 2.1 Over all of micro hydropower plant with penstock [7] shows an over all of the micro hydropower system; the water in a running river is diverted into a canal through the intake. It will form a forebay which is a settling tank to hold the flowing water. The penstock or pipe then will lead the water into the mechanical turbine and rotates the shaft. This rotation then will be utilized by the generator to produce electric power that either is used by local loads or is delivered to the electric

power network [7].

The power that can be accessed from the water is determined by two characters of the water. The first thing is head which is the vertical difference between the front of water conveyance and the turbine. The second point is the flow which is the mass of falling water. The power generated by micro hydropower depends largely on the head and the flow rates available. The actual power produced may differ depending on turbine and generator efficiency and pressure losses through the intake and penstock. Mathematically power from micro hydropower plant is given by

$$P=\eta gQH \qquad 2.1$$

where η , g, Q and H are overall efficiency, gravitational acceleration, mass flow of water and head respectively [8]. Such a small-scale hydropower system is suitable for a homeowner and small business owners who have access to the flowing water with a relatively high head (3 feet or above) but located in remote communities.

Development of micro hydropower systems requires selection of the proper turbines and generators. The components of micro hydropower plant are shown in figure 2.1. Moreover, the control systems should be designed for grid connection of micro hydropower plants.

2.3.1 Electro Mechanical Components

Electro mechanical components are the powerhouse components of micro-hydropower and they are used to convert mechanical energy of water into electrical energy. The main electro mechanical components of a micro hydro plant are the turbine, valve, generator and drive systems.

Turbines

The characteristics of the micro hydro power turbine are critical in micro hydropower plant design. It converts the energy from the running water to a whirling mechanical energy form which can be used by the generator. There are two main types of hydro turbine: impulse turbines and reaction turbines.
Impulse turbines have fixed nozzles which will eject the water and directly shoot it on the turbine moving buckets. The direction of the water will be changed resulting in the turbine spin. The kinetic energy loss in flowing water will in part convert to the mechanical energy of turbine. Typical impulse turbines are:-Pelton wheels turbines, water wheels and cross flow (Banki) turbine [9].

Reaction turbines extract energy from the water by decreasing the pressure, angular momentum, and velocity of the fluid. Fluid pressure changes after flowing out of the rotating nozzle on the rotor. They are more appropriate for low head flow but high flow velocities condition. Typical impulse turbines are:- Francis turbines and Kaplan turbines.

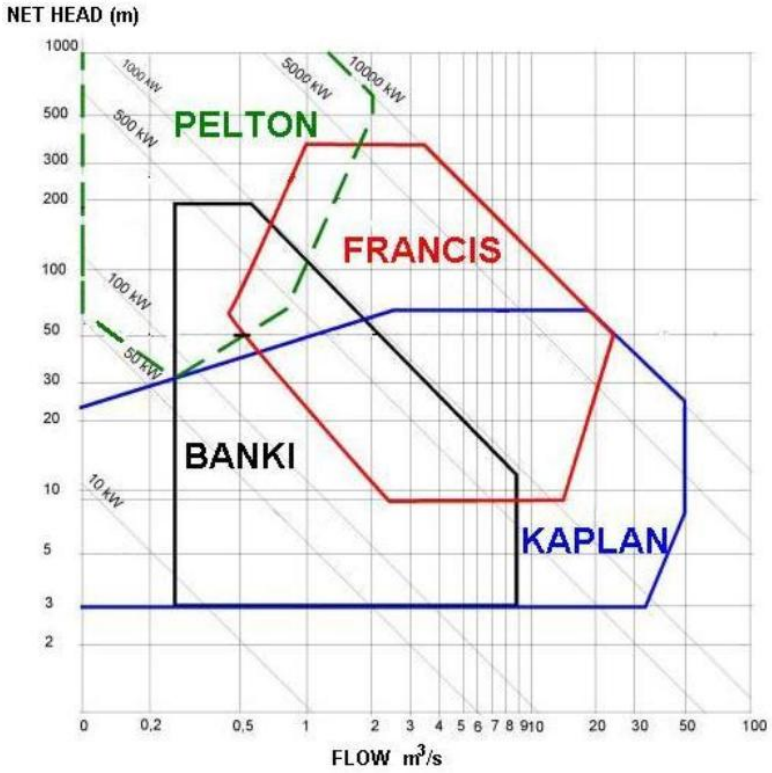

Figure 2. 2 Range of head and flow rate for different types of hydro power turbine operation [9].

The figure 2.2 shows suitable hydro power turbine choice under the different head and flow conditions. The Pelton turbine is appropriate for the state that the head is higher than 30m, the flow rate is lower than 2 m^3/s and total power greater than 50 kW. The Francis turbine which occupies the central part of the graph should run at 8-400 m head, 0.5-25 m^3/s and the power rating of 250 kW - 10 MW. The Banki turbine working area is under 200m head, 0.3-9 m^3/s flow rate and less than 1MW. The Kaplan turbine can run at 50 m^3/s flow rate at most with a maximum 70m head and 10MW power.

For traditional hydro plants, Pelton and Francis will be a good choice because of their large power and head capacities. However, for a MHPP which means the rating power is less than 500Kw, the Kaplan turbine has the largest operation area compared to others. It is also the only turbine that can

work below 10Kw power rating. Based on these considerations, Kaplan turbine is the best choice of our micro hydropower turbine for power generation [9].

Advantages of Kaplan turbine

- Its efficiency can be up to 95%.
- Can be applied in low head conditions allowing for power plants at lower height.
- The variation of its size and output allows it for MHPP instead of large dams.
- It is comparatively low cost due to the small size and low head requirements.
- Dams construction with this turbine design produces less ecological impact because it requires low head, the reservoir area would not be flooded as much as high head dams.

Generator

Generator is a device that converts mechanical power into electrical power to produce electricity based on the principle of electromagnetic induction. Generators basically divided in two known as DC (direct current) generators and AC (alternating current) generators [10].

DC generator is typically found in off-grid applications. It gives a power supply directly into electric storage devices and DC power grids without novel gear and the stored power is carried to loads by using dc-ac converters. As batteries tend to be stimulating to recover considerably more fuel, the DC generators could be controlled back to a motionless speed [10].

AC Generators is the most significant means of generating electrical energy in many of the areas because now days all the clients are using AC. These are two types of AC generator: induction generator and synchronous generator. The induction generator also known as Asynchronous Generators, does not requires separate DC excitation, regulator controls, frequency control or governor. The generators should run at a consistent speed to transmit a stable AC voltage, even at no load condition. These are generally used in small machines like mixer grinders, and as large machines used in Industries [10].

Synchronous generators are large size generators which rotates at synchronous speed and mainly used in power plants because of its high efficiency. These may be rotating field type or rotating armature type. Armature is at rotor and field is at stator for the rotating armature type. Rotor

armature current is taken through slip rings and brushes . These are restricted due to high wind losses. These are used for low power output applications. Rotating field type of alternator is widely used because of high power generation capability and nonappearance of slip rings and brushes [10].

2.4 Pulse Width Modulation

In electronic power converters and motors, PWM is used extensively as a means of powering alternating current (AC) devices with an available direct current (DC) source or for advanced DC /ACconversion. Variation of duty cycle in the PWM signal to provide a DC voltage across the load in aspecific pattern will appear to the load as an AC signal, or can control the speed of motors that would otherwise run only at full speed or off [11].

The duty cycle of a PWM signal varies by using the pattern that can be created through simple analog components, a digital microcontroller, or specific PWM ICs. In an Analog PWM control both reference signals and carrier signals that are feed into a comparator need to be generated to creates output signals based on the difference between the signals. Sinusoidal signal is a reference signal and it is at the frequency of the preferred output signal, as either a saw tooth or triangular wave at a frequency significantly larger than the reference is often the carrier signal. When the carrier signal becomes greater than the reference signal, the comparator output signal is at one state, and when the reference signal is at a higher voltage, the output is at its second state. This process is shown in Figure 2.3 with the triangular carrier wave in red, sinusoidal reference wave in blue, and modulated and un modulated sine pulses [11].

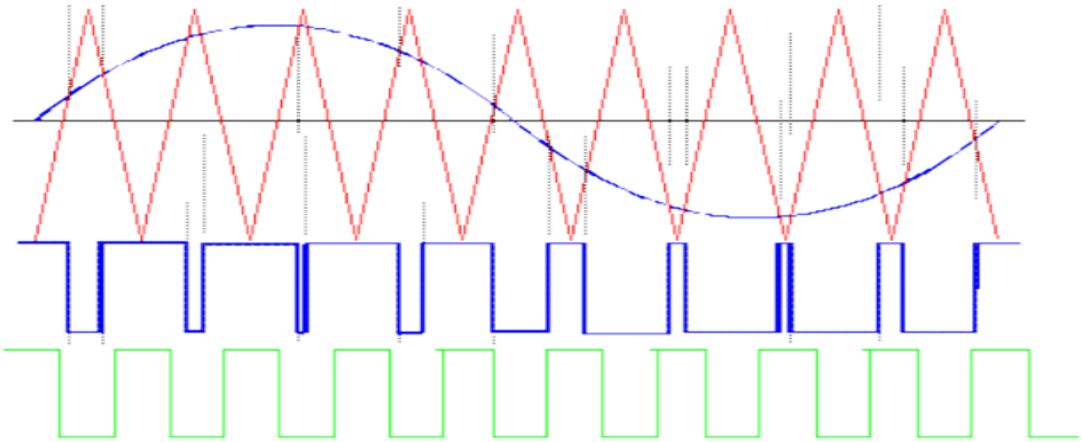

Figure 2. 3 The triangular carrier wave (red), sinusoidal reference wave (blue), and modulated and un modulated sine pulses [11].

2.5 Phase locked loop for grid synchronization

The integration of large scale wind, solar power and micro hydropower systems to the grid is a growing trend in modern power system. The viability of this technique is in the ability to match the renewable energy resources with the running network with proper control strategy. Phase lock Loop is vital for control and tracking of phase and frequency of the incoming signal of grid connected systems such as distributed generation [12].

The frequency and the phase signal must be extracted in order to track the phase of any signal. The system composed essentially of three parts such as; the phase detector (PD), the low pass filter (LPF) and the voltage controlled oscillator (VCO). An output signal which is the phase difference of the input signal ϕ-in, and the signal generated by the internal oscillator of the PLL ϕ-out was generated by the phase detector. On the other hand, the LPF attenuates the high frequency AC components from the PD output. The VCO generates at its output an AC signal whose frequency is shifted with respect to a given central frequency ωc, as a function of the input voltage provided by the LPF [13]

The following are the three main categories of PLL structures [14]:

- Zero crossing detection (ZCD)
- Stationary reference frame
- Synchronously rotating reference frame (SRF) based PLL

The major limitations with some of the approaches are, firstly, the ZCD based PLL in the reviewed literature is although the simplest but its performance becomes poorer if frequency variation or line notching is present. Conversely during unbalanced voltage condition stationary reference frame based PLL structure is not capable of accurate phase tracking. As grid connected systems experience problems such as flicker, dip, improper phase jump, input phase shift, amplitude variation, notch and several others, this work adopted the synchronously rotating reference frame (SRF) based method of PLL design to synchronize a micro hydro power generation with the grid under different perturbation, so as to improve the power quality. In order to achieve this, a typical synchronous reference frame phase lock loop is represented in figure 2.4 [14].

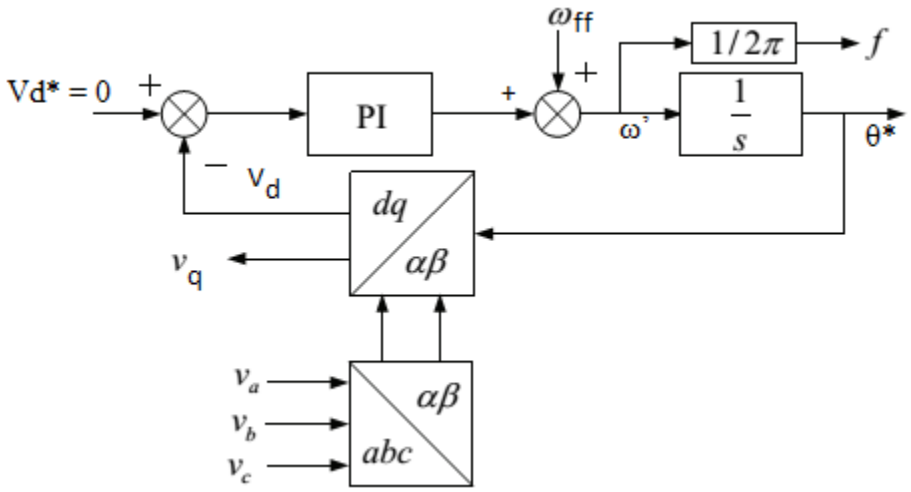

Figure 2. 4 Basic structure for the SRF PLL system

In figure 2.4 the phase voltages *Va, Vb* and *Vc* are obtained from sampled phase voltages from the grid and inverter output terminal. These stationary reference frame voltages are then transformed to voltages *Vd, Vq* (in a frame of reference synchronized to the utility frequency) using *αβ* and *dq* transformation. The αβ transformation allows to represent three phase system *Va, Vb* and *Vc* as two phase Vα and Vβ. The control in αβ frame has the feature of reducing the number of required control loops from three to two [15]. However, the reference and feedback signals are in general sinusoidal functions of time. Therefore, to achieve a satisfactory performance and small steady state errors in

magnitude and phase, the compensator design is not straight forward task. The d-q frame based control offers a solution to this problem.

2.5.1 Stationary reference frame αβ

To track the phase angle the three phase voltage signals Va, Vb and Vc are transferred from three phases to a stationary system of two phases Vα and Vβ. The grid voltages are expressed as follows [14]

$$V_a = V_m \sin(\theta) \quad 2.2$$

$$V_b = V_m \sin(\theta - \frac{2\pi}{3}) \quad 2.3$$

$$V_c = V_m \sin(\theta + \frac{2\pi}{3}) \quad 2.4$$

where θ is the phase angle 2πft. The αβ-transformation matrix is given in equation (2.5) [14].

$$T_{\alpha\beta} = \frac{2}{3}\begin{bmatrix} 1 & -\frac{1}{2} & -\frac{1}{2} \\ 0 & -\frac{\sqrt{3}}{2} & \frac{\sqrt{3}}{2} \end{bmatrix} \quad 2.5$$

Carrying out the matrix multiplication $V\alpha\beta = T\alpha\beta * Vabc$, we can get:

$$\begin{bmatrix} V_\alpha \\ V_\beta \end{bmatrix} = \begin{bmatrix} V_m \sin(\theta) \\ V_m \cos(\theta) \end{bmatrix} \quad 2.6$$

which is two signals carrying information only about the phase angle of one of the phases, Va.

2.5.2 Synchronous rotating reference frame based PLL

The phase angle θ is tracked by synchronizing the voltage space vector along q or d axis in the SRF [14]. Here the voltage space vector is synchronized with the q-axis as shown in figure 2.5.

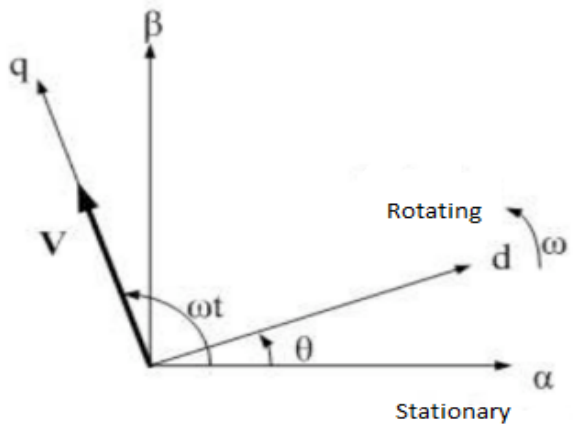

Figure 2. 5 Synchronous rotating reference frame [14]

If the voltage space vector is to be synchronized with the q-axis the transformation matrix is

$$T_{qd} = \begin{pmatrix} \text{Sin } \theta^* & \text{Cos } \theta^* \\ -\text{Cos } \theta^* & \text{Sin } \theta^* \end{pmatrix} \quad 2.7$$

where θ* is the estimated phase angle output of the PLL system. Carrying out the transformation Vqd = Tqd *Vαβ and using the trigonometric addition formulas yields [16].

$$\begin{pmatrix} V_q \\ V_d \end{pmatrix} = \begin{pmatrix} V_m \cos(\theta - \theta^*) \\ -V_m \sin(\theta - \theta^*) \end{pmatrix} \quad 2.8$$

The phase angle θ is estimated with θ* which is the integral of the estimated frequency ω'. The estimated frequency ω' is the sum of the PI-output and the feed forward frequency ωff. Gains of the PI-regulator is then designed so that Vd follows the reference value Vd* = 0, as shown in figure 2.4. If Vd = 0 then the space voltage vector is synchronized along the q-axis and the estimated frequency ω' is locked on the system frequency ω. This results in an estimated phase angle θ* that equals the phase angle θ [13]. If $\theta^* \approx \theta$ then the small angle approximation for sin function yields Vd = -Vm(θ–θ*) and the structure in figure 2.4 can be simplified to figure 2.6.

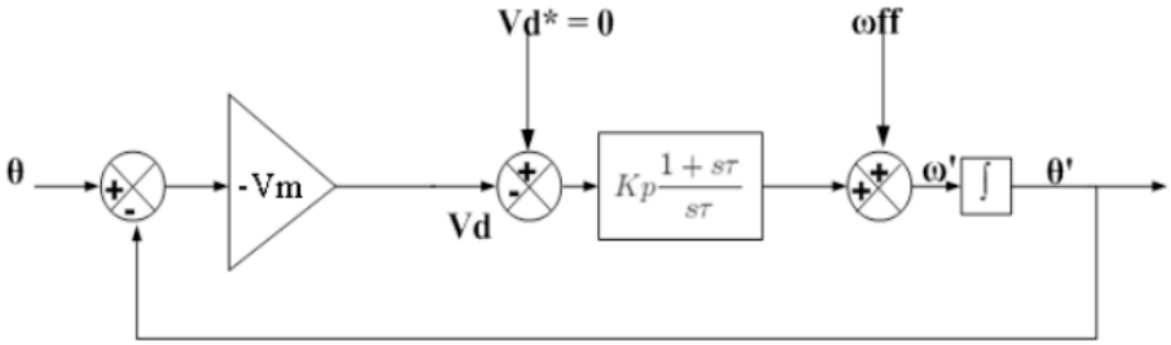

Figure 2. 6 Simplified system for the SRF PLL.

The purpose of the feed forward frequency, ωff, is to have the PI-regulator control for an output signal that goes to zero. In our case the feed forward frequency is $2\pi f = 100\ \pi$ rad/s. In the ideal case when the grid frequency is exactly 50Hz once the regulator has tracked the phase the output of the regulator becomes zero.

2.6 Previous Works on Grid Connected of Micro Hydropower Plant

In 1993, D. S. Henderson and D. E. Macpherson presented a novel control method of electronic load governor for a micro hydro generator to balance the generator power production and the user's load requirement. Unlike the traditional speed governors which maintain the generator speed by adjusting the water flow, the paper proposed electronic load governor for speed adjustment. Switching devices are used for switching on or off the ballast load to balance the system. In this article, the balance is achieved, but specific topology or algorithm of the switching devices was not given. Some other stand-alone micro hydropower research based on induction generator shared the same idea with D. S. Henderson and D. E. Macpherson that compensate the load differences by manipulating the switching circuit of the ballast load [17].

In 2014, D. Melly, R. Horta, C. Münch, H. Biner, S. Chevailler designed two permanent magnet machines along with AC-DC converter for a new axial counter-rotating turbine [18]. The DC bus voltage control is done by a rectifier topology called Vienna rectifier. Such a control strategy has great robustness, high power density, a low blocking voltage stress on power semiconductors and sinusoidal current requirement. By the experimental results of the turbine prototype, it showed a stable control of the system with high efficiency [19].

Khalid Tourkey Atta, Andreas Johansson, Michel J. Cervantes, and Thomas Gustafson [20] proposed a maximum power point tracking method for the micro-hydropower turbine. Extremum

seeking control is discussed in this paper. The simulation results of the algorithm were demonstrated, and the experimental data of the whole system showed the possibility of using this algorithm in the micro hydropower plant. The typical structure of micro hydropower system should use PMSG with an AC-DC-AC energy converter as mentioned in their paper. However, the generator utilized in the experiment is a Siemens DC machine which is connected to the grid through a DC converter [20].

In this research, power electronics and PLL for MHPP are designed and PMSG was used. PMSG is a very efficient electric machine which is broadly used in renewable power generation nowadays. Unlike the traditional synchronous generator, the source of the field of magnetic material in PMSG is the permanent magnetic material. Such a moveable magnetic field can eliminate field exciting winding in the rotor which means less copper loss and mechanical commutator, brushes or slip rings are not needed in PMSG. The absence of these components brings less loss, smaller size, more controllability and more convenient maintenance for PMSG. The three phase full bridge diode which is unidirectional power converter is used in (PMSG) based system. To match up with the DC linkage voltage boost converter which step up the dc voltage is used [21].

CHAPTER THREE

MICRO HYDRO POWER TURBINE AND PERMANENT MAGNET SYNCHRONOUS GENERATOR MODELING

3.1 Modeling of micro hydro power turbine

As discussed in chapter two, Kaplan turbine is selected for micro hydropower generation. It is a reaction turbine with propeller (runner blades) and wicket gate which can adjust the water flow. The water flows directly to wicket gate and is perpendicular to the propeller. The water falls through runner blades because of the gravity force and cause the turbine to spin.

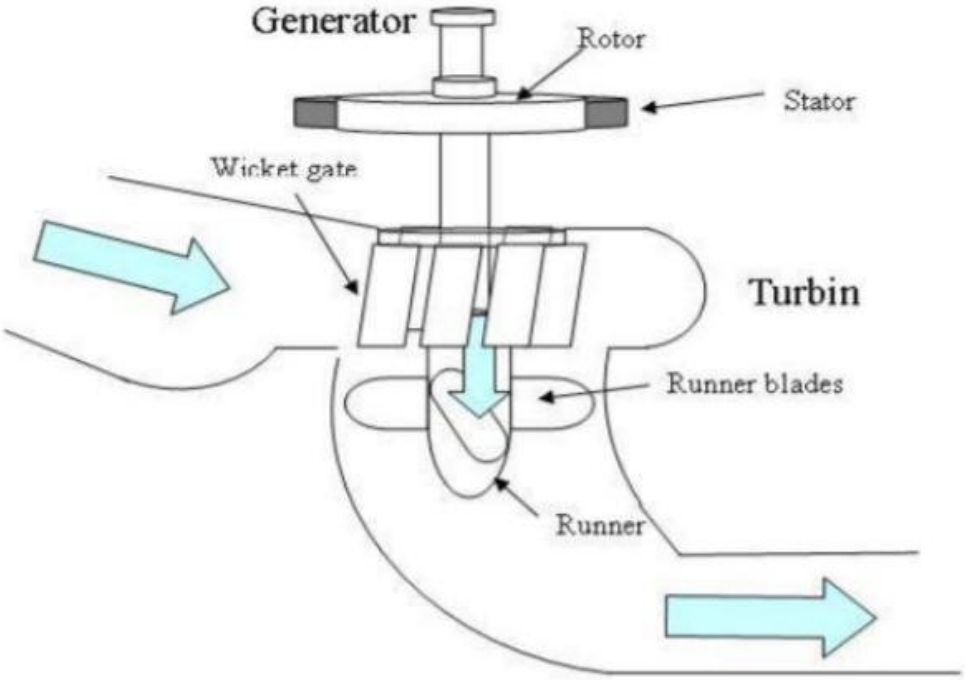

Figure 3. 1 Insight view of Kaplan turbine operation principle with a generator [22].

A specially designed nozzle is the outlet of water which can decelerate the water speed. The decrement of speed will lower the pressure on the outlet side. Thus, the difference of pressure between inlet and outlet will increase which can increase the water flow through the blades and

extract more power from the water. The available output hydropower can be expressed as follows [22]:

$$P_{hydro} = \rho * g * H * Q \quad (3.1)$$

Where ρ is density of the water (kg/m^3), g is the gravity acceleration (m/s^2), H is the head of water (m), and Q is volume flow rate of water (m^3/s). The turbine efficiency is shown as follows:

$$\eta_t = \frac{P_t}{P_{hydro}} \quad (3.2)$$

where: P_t is Power output of turbine

η_t is turbine efficiency

$$P_t = \tau * \omega \quad (3.3)$$

τ is the torque of the turbine and ω is the rotation speed of the turbine.

3.1.1 A simplified model of the hydro turbine.

Essential design criteria for the turbine are:

- net head available
- flow speed of the water
- required speed used for coupling to a generator

A turbine is characterized by its power-speed- and efficiency-speed- characteristics. This means that for a particular head, a turbine runs most efficiently at a particular speed and therefore requires a particular flow.

For the analysis, purpose Huluka river was selected with head of 14m [23] and flow speed of 0.244 m3/sec, therefore, kaplan turbine is the most convenient one.

Mean Monthly Flow Rate of Huluka River (Ministry Of Water, Irrigation and Energy (MOWIE), 1997)

Table 3. 1 Mean Monthly Flow Rate of Huluka River *(MOWIE)*

Month	**Water flow rate**
January	0.489
February	0.37
March	0.526
April	0.276
May	0.094
June	0.25
July	2.199
August	2.631
September	0.8
October	0.356
November	0.244
December	0.103
Annual Average	**0.695**

Comparison of flow rates by their profit is shown in table 3.2 below. Investment cost is approximately 0.06 dollar per Kwh (around 1.80birr/Kwh).

Table 3. 2 Comparison of flow rates by their profit

Q(m^3/s)	**Power (Kw)**	**Revenue (birr/year)**	**Investment cost (birr/year)**	**Profit (birr/year)**
0.094	11.62	244,457.16	183,206.815	61,250.35
0.103	12.73	262,940.35	197,976.96	64,963.39
0.244	30	535,530.5	466,560	68,970.5
0.25	30.9	549,410.5	480,556.8	68,853.7
0.276	34.22	597,402.908	532,144.34	65,258.6

Revenue was calculated by using the Ethiopian Electric Utility tariffs as shown in table 3.3 below.

Table 3. 3 Ethiopian Electric Utility tariffs

Energy (Kwh)	Tariff (birr)
Up to 50	0.273
51 - 100	0.767
101 - 200	1.625
201 - 300	2
301 - 400	2.2
401 - 500	2.405
> 500	2.481

As indicated in table 3.2, the profit at the flow rate of $0.244m^3/s$ is the highest. So, the turbine and generator were modeled for 30KW to have this advantage. In addition, the modeled turbine and generator also operate at the flow rates of $0.094m^3/s$ and $0.103m^3/s$. However, at these flow rates turbine and generator were inefficient because they operate under their capacity.

Once an appropriate turbine is selected, its speed should be reconciled with the speed of the generator, or with any other machine that is mechanically driven by the turbine. If the turbine and generator speeds are different, gearing, a belt or chain drive between turbine and generator is required. The generator speed [rpm] is calculated according to:

$$rev = \frac{120 * f}{P} \qquad 3.4$$

where rev = revolution per minute [rpm]

f = frequency [Hz]

P = poles number

For a commonly used alternator, for 50 Hz and with 4 poles, a speed of 1500 rpm is calculated.

3.1.2 Linear Turbine modeling

The hydraulic turbine and water columns' linear modeling is usually based on the following assumption [24].

1. The hydraulic resistance is negligible.
2. The penstock pipe is inelastic and water is incompressible.
3. The turbine output power is proportion to the product of head and volume flow.

In micro hydropower systems, hydraulic turbines are used to derive permanent magnet synchronous generators. These hydraulic turbines convert the energy of flowing water into mechanical energy which in turn is converted into electrical energy. The hydraulic turbine is already modeled in different literatures. Figure 3. 2 shows the use of turbines with varying head as shown below [25].

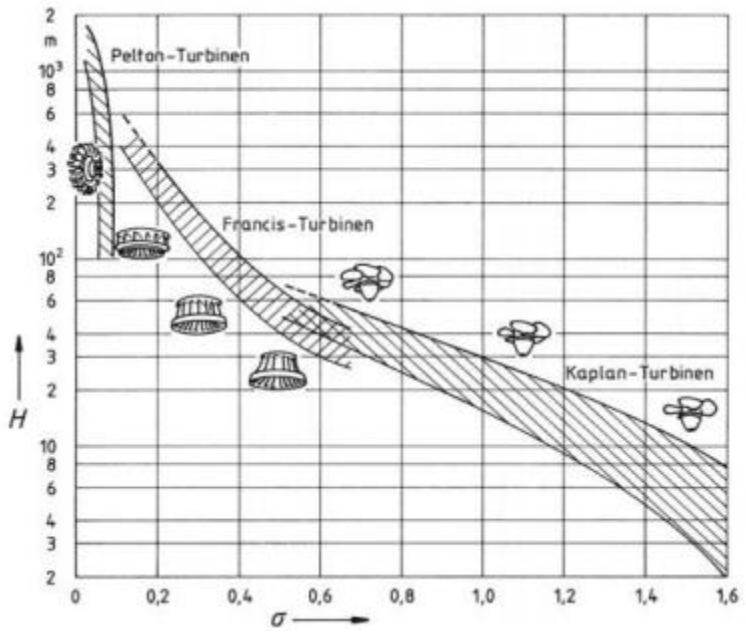

Figure 3. 2 The use of turbines with varying head [25]

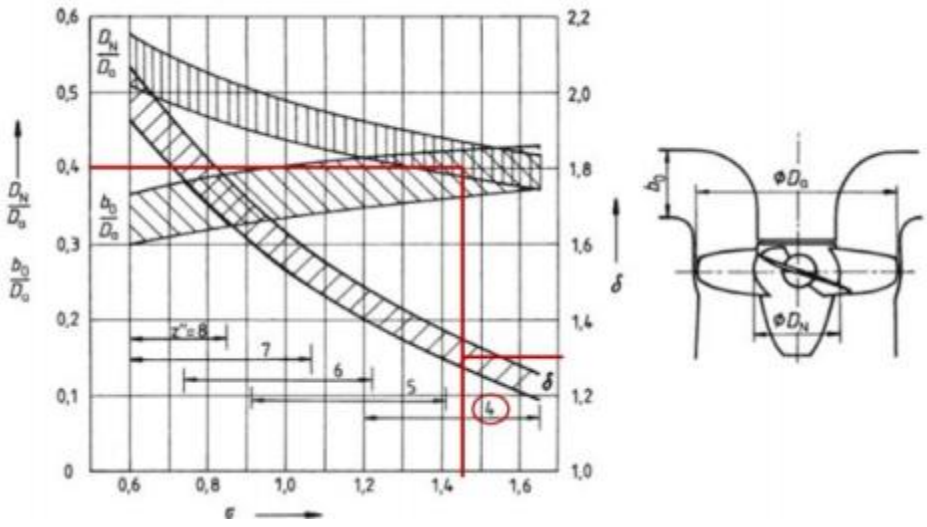

Figure 3. 3 Design diagram for a Kaplan turbine [25]

The rotational speed N of the turbine is given by equation (3.4) [25].

$$N = \frac{\sigma(2gH)^{3/4}}{2\sqrt{\prod Q}} \quad 3.4$$

Then, the specific speed is obtained as

$$Ns = \frac{N\sqrt{Q}}{H^{3/4}} \quad 3.5$$

$$P_t = \rho\frac{1}{4}\prod(D_a{}^2 - D_N{}^2)C_o u\Delta w_u \quad 3.6$$

where,

D_a = inner diameter of the wheel

$$D_a = \frac{2\delta}{\sqrt{\prod}}\sqrt[4]{\frac{Q}{2gH}} \quad 3.7$$

D_N =outer diameter of the wheel

δ =diameter number of 2 is related to σ =0.65 and diameter ratio ($\frac{D_N}{D_a}$) of 0.5

Thus, $D_N = D_a * 0.5$

C_o = Relative velocity in meridian direction

$$C_o = \frac{Q}{A} = \frac{Q}{\frac{1}{4}\prod(D_a{}^2 - D_N{}^2)} \quad 3.8$$

u = Tangential velocity of the blade

$$u = \prod D_a N \quad 3.9$$

Δw_u = Difference of the tangential velocity

$$\Delta w_u = w_{u1} - w_{u2} = \frac{Hg\eta_e}{u} \quad 3.10$$

where

w_{u1} = Tangential velocity at the leading edge

w_{u2} = Tangential velocity at the trailing edge

Using equation 3.2 the expression for torque can be written as shown in equation 3.11.

$$\tau = \frac{P_t}{\omega} = \frac{\rho \frac{1}{4} \prod (D_a{}^2 - D_N{}^2) C_o u \Delta w_u}{\omega} \qquad 3.11$$

3.2 Modeling of permanent magnet synchronous generator

3.2.1 Introduction of PMSG

The beginning of PMSG can date back to 1930 when the alnico magnet was discovered. The application of PMSG was limited by the undeveloped semiconductors because power converters play a key role in variable frequency and speed generator circuits. People started to pay more attentions to PMSG application with the progress of key technologies like permanent magnet material, control theory and semiconductor component [26].

PMSG is a very efficient electric machine which is widely used in renewable power generation nowadays. Unlike the traditional synchronous generator, the source of the magnet field in PMSG is the permanent magnet material. Such a moveable magnet field can eliminate field exciting wind in the rotor which means less copper loss and mechanical commutator, brushes or slip rings are not needed in PMSG. The absence of these components brings less loss, smaller size and more convenient maintenance for PMSG [26].

Heat up problem will only happen on the stator which is easier to cool down because no current is needed to excite magnet field on the rotor. In the micro hydropower system, PMSG is selected for the following advantages: higher power density, less maintenance is needed, greater controllability with the elimination of mechanical brushes [26].

Before we model the PMSG, the following assumptions are applied:

1. Magnetic saturation is negligible.
2. Induced EMF is sinusoidal.
3. Eddy current and hysteresis losses are negligible.
4. Damping effect is negligible.

3.2.2 Mathematical model of PMSG in natural ABC frame

Figure 3.4 shows the cross view of the three phase, two poles PMSG. The ABC windings in the stator are 120^0 electric angle from each other and the magnetomotive force (MMF) f_a, f_b and f_c represent the stationary directions. The d axis represents the flux direction of the permanent magnet which is rotating at the speed ω_m. θ_r stands for the angle between the flux direction (d-axis) and the stationary a-axis [27].

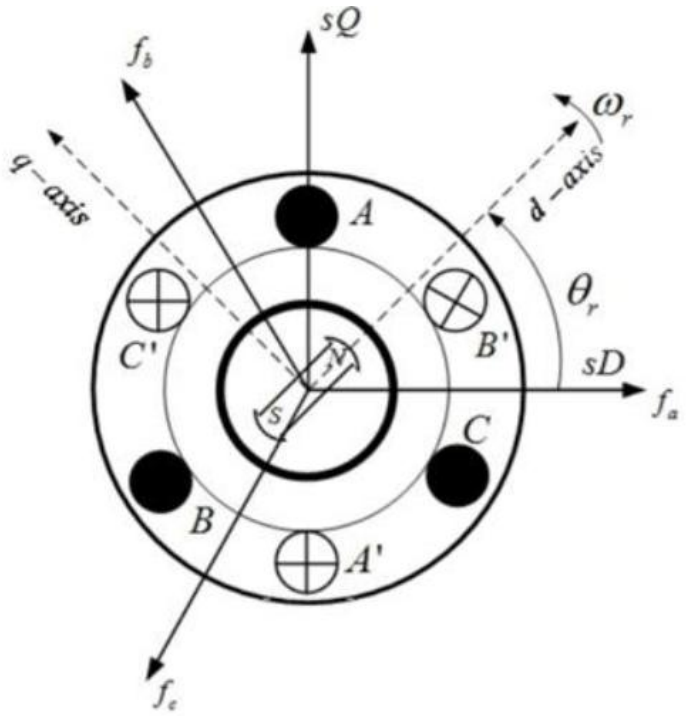

Figure 3. 4 Cross view of three phase PMSG with a single pole pair [27]

The stator voltage equations of PMSG in ABC frame regarding phase current and flux linkages can be written as follows [27].

$$\begin{bmatrix} V_a \\ V_b \\ V_c \end{bmatrix} = \begin{bmatrix} Rs & 0 & 0 \\ 0 & Rs & 0 \\ 0 & 0 & Rs \end{bmatrix} \begin{bmatrix} ia \\ ib \\ ic \end{bmatrix} + \frac{d}{dx} \begin{bmatrix} \lambda a \\ \lambda b \\ \lambda c \end{bmatrix} \quad 3.12$$

Where Va, Vb and Vc are stator instantaneous voltages in ABC phase and ia, ib and ic are stator instantaneous currents in ABC phase. Rs is the stator winding resistance in ABC phase. λa, λb and λc are flux linkages induced by the AC currents and the permanent magnet. The detail expression

can be expanded as follows [10]:

$$\begin{bmatrix}\lambda a\\ \lambda b\\ \lambda c\end{bmatrix} = \begin{bmatrix}Laa\ Lab\ Lac\\ Lba\ Lbb\ Lbc\\ Lca\ Lcb\ Lcc\end{bmatrix} \begin{bmatrix}ia\\ ib\\ ic\end{bmatrix} + \lambda_m \begin{bmatrix}\cos(\omega_m)\\ \cos(\omega_m - \frac{2\pi}{3})\\ \cos(\omega_m + \frac{2\pi}{3})\end{bmatrix} \quad 3.13$$

Where Laa, Lbb, and Lcc are self-inductance of ABC phase and Lab, Lac, Lba, Lbc, Lca and Lcb is mutual inductances respectively for ABC phase. λm is the flux linkage formed by the permanent magnet material. As we can see from the equation, both self-inductances and mutual inductances are all functions of rotating speed ωm. Such a varying time characteristic of inductance causes the difficulty in calculation and analysis. Thus, d-q axis modeling is needed as given in section 3.2.3.

3.2.3 Mathematical model of PMSG in rotational d-q frame

R.H. Park first introduces the dq0 Park's transformation to simplify the synchronous machine models. In the stationary ABC frames of PMSG, the main phase quantities like stator voltages, currents, and flux linkages are time dependent. The 3-phase machine is analyzed by rotational two-axis. Direct-axis is on the rotor magnetic flux direction and quadrature-axis is perpendicular to direct-axis. Under this d-q frame, the varying time characteristic of phase quantities can be eliminated. The ABC to dq0 transformation is shown as follows [10]:

$$\begin{bmatrix}Vd\\ Vq\\ V0\end{bmatrix} = \frac{2}{3}\begin{bmatrix}\cos(\omega_m t) & \cos(\omega_m t - \frac{2\pi}{3}) & \cos(\omega_m t + \frac{2\pi}{3})\\ -\sin(\omega_m t) & -\sin\left(\omega_m t - \frac{2\pi}{3}\right) & -\sin(\omega_m t + \frac{2\pi}{3})\\ \frac{1}{2} & \frac{1}{2} & \frac{1}{2}\end{bmatrix} * \begin{bmatrix}Va\\ Vb\\ Vc\end{bmatrix} \quad 3.14$$

The inverse transformation:

$$\begin{bmatrix}Va\\ Vb\\ Vc\end{bmatrix} = \begin{bmatrix}\cos(\omega_m t) & -\sin(\omega_m t) & 1\\ \cos\left(\omega_m t - \frac{2\pi}{3}\right) & -\sin\left(\omega_m t - \frac{2\pi}{3}\right) & 1\\ \cos\left(\omega_m t + \frac{2\pi}{3}\right) & -\sin\left(\omega_m t + \frac{2\pi}{3}\right) & 1\end{bmatrix} * \begin{bmatrix}Vd\\ Vq\\ V0\end{bmatrix} \quad 3.15$$

Vdq0 represents the voltages on the d-q rotational frame. The transformation can also be applied to the stator current and flux linkages for AC synchronous machine. For a balanced ABC stationary frame condition, Va+ Vb +Vc=0. Thus V0=0 after the Park transformation. By combining the ABC frame model and d-q transformations, the PMSG modeling in d-q axis can be expressed as follows [27]:

$$V_d = i_d R_s + L_d \frac{di_d}{dt} - \omega_e L_q i_q \quad 3.16$$

$$V_q = i_q R_s + L_q \frac{di_q}{dt} + \omega_e L_d i_d + \omega_e \lambda_m \quad 3.17$$

$$V_o = i_o R_s + L_o \frac{di_o}{dt} \quad 3.18$$

where Vd,Vq, Id, Iq, Ld, Lq represent the voltage, current, and inductance respectively in the rotational d-q axis. λm is the linkage of flux produced by the permanent magnet material. ω_e is the electrical rotation speed of the PMSG. The corresponding circuit in the d-q edge can be obtained from the above equations as shown below:

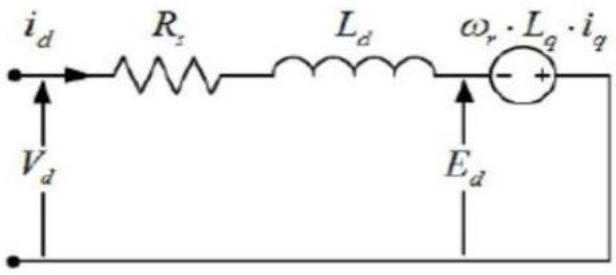

Figure 3. 5 Equivalence circuit of PMSG in d-axis [10].

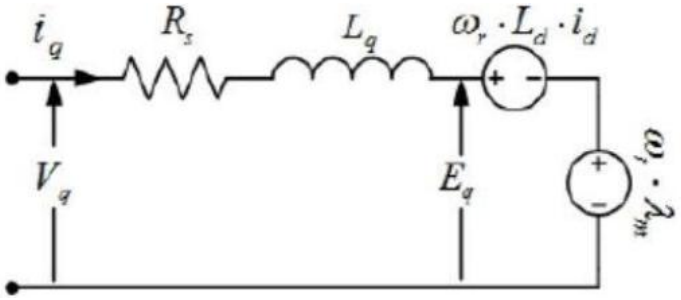

Figure 3. 6 Equivalence circuit of PMSG in q-axis [10].

Where Ld, Lq are synchronous inductance. They are almost equal in the surface mounted PMSGs [28]:

$$L_d = L_q = \frac{2}{3}L \tag{3.19}$$

Where L is the total inductance tested by the serial-parallel connecting of the stator.

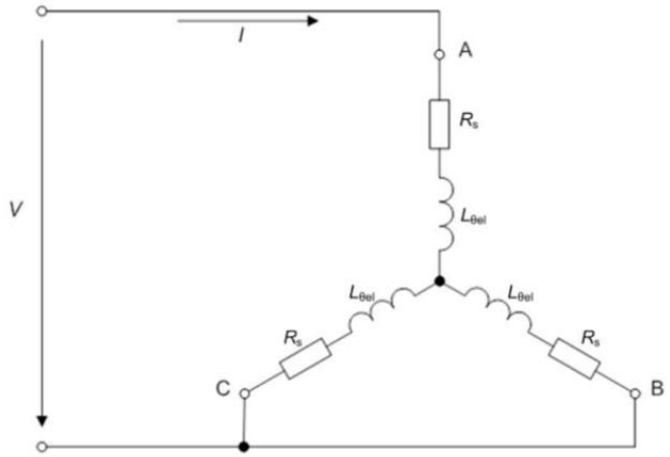

Figure 3. 7 Serial-parallel testing circuit for the generator inductance [28]

3.2.4. Electrical torque and power analysis

Ed and Eq are back electromotive force (EMF) in d-q axis respectively and can be written as

$$E_d = -\omega_e L_q i_q = -\omega_e \lambda_q \tag{3.20}$$

$$E_q = \omega_e L_d i_d + \omega_e \lambda_m = \omega_e \lambda_d \tag{3.21}$$

The mechanical power generated by the PMSG expressed by the d-q axis voltage and current can be expressed as follows:

$$P_m = \frac{2}{3}(E_d i_d + E_q i_q) \tag{3.22}$$

By substituting equation (3.20) and (3.21) in to equation (3.22), it gives:

$$P_m = \frac{2}{3}(\omega_e \lambda_d i_q - \omega_e \lambda_q i_d) \quad 3.23$$

$$T_e = \frac{3}{2}(\frac{p}{2})(\lambda_d i_q - \lambda_q i_d) \quad 3.24$$

Where T_e is the electromagnetic torque, ω_m is the mechanical rotation speed, and p is the total number of poles. Thus, from the equation the electromagnetic torque expressed by the d-q axis elements can be written as [27]:

$$T_e = \frac{P_m}{\omega_m} = \frac{P_m}{\omega_e}(\frac{p}{2})$$

Or

$$T_e = \frac{3}{2}(\frac{p}{2})(\lambda_m i_q - (L_q - L_d) i_q i_d) \quad 3.25$$

Since we have assumed that Ld=Lq, the torque equation can be further simplified as follows:

$$T_e = \frac{3}{2}(\frac{p}{2})\lambda_m i_q \quad 3.26$$

CHAPTER FOUR

MHP CONVERTERS AND CONTROL COMPONENT DESIGN

4.1 AC to DC Rectifier

Rectifiers are used to convert the AC sine wave voltage with 50 or 60 Hz frequency to a DC voltage with ripple. In micro hydropower system two types of AC-DC rectifiers are commonly used. The first one is active PWM rectifiers and the second one is diode rectifiers. The semiconductor components used in active rectifiers are IGBT and diode which can work as both inverter and full bridge rectifiers by manipulating IGBT switches [29]. Such a topology is frequently used in doubly fed induction generator based system. Thus, it is not going to be employed in this research because of the generator type in the system [29].

The second rectifier which is used in this thesis is diode rectifiers. Unlike the PWM rectifiers, we have no control of the output voltage of the rectifier because diodes are passive semiconductor components which do not have a switch to turn on or off [30].

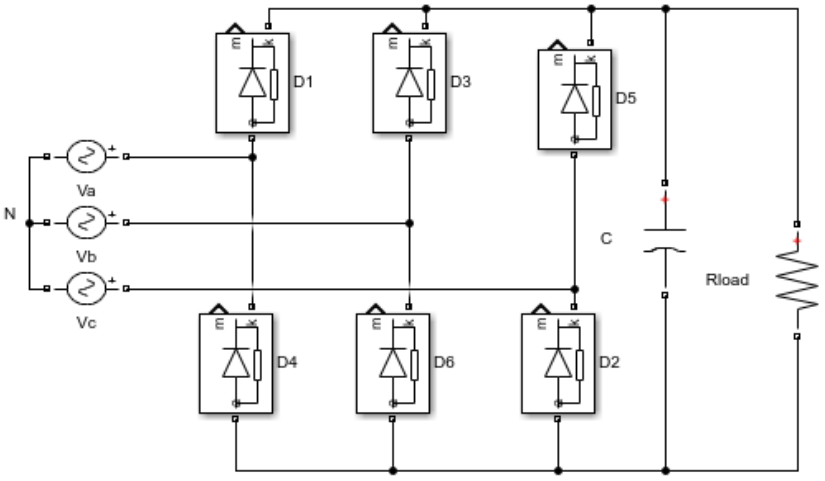

Figure 4. 1 Three phase full bridge diode rectifier [30] .

The diode unidirectional conduction characteristic ensures the power will only flow from the AC side to the DC side. This topology will bring massive current distortion of AC side. If the AC source is from the utility, the current distortion problem needs to be considered. However, in this micro

hydropower system, the current distortion will not cause as many troubles as it does on the utility grid. Thus, this uncontrolled rectifier is used to be the AC-DC converter because of its unidirectional conducting and simplicity [30].

The diodes are numbered in the order of their conduction sequences and the conduction angle of each diode is 2π/3. 1-2, 2-3, 3-4, 4-5, 5-6, and 6-1 are the conduction order for diodes. The waveforms of the 3-Φ bridge rectifier for both voltage and current are shown in figure 4.2.

The average value of the output can be found as [30]:

$$V_{DC} = \frac{6}{2\pi}\int_{\frac{\pi}{3}}^{\frac{2}{3}\pi} \sqrt{3}V_s Sin(wt)d(wt) = \frac{3\sqrt{3}}{\pi}V_s = 1.654V_s \qquad 4.1$$

Similarly, the rms value of the output voltage can be found as:

$$V_L = \left(\frac{9}{\pi}\int_{\pi/3}^{\frac{2\pi}{3}} V_s^2 \mathrm{Sin}^2(wt)\,d(wt)\right)^{\frac{1}{2}} = V_s\left(\frac{3}{2}+\frac{9\sqrt{3}}{4\pi}\right)^{\frac{1}{2}} = 1.655V_s \qquad 4.2$$

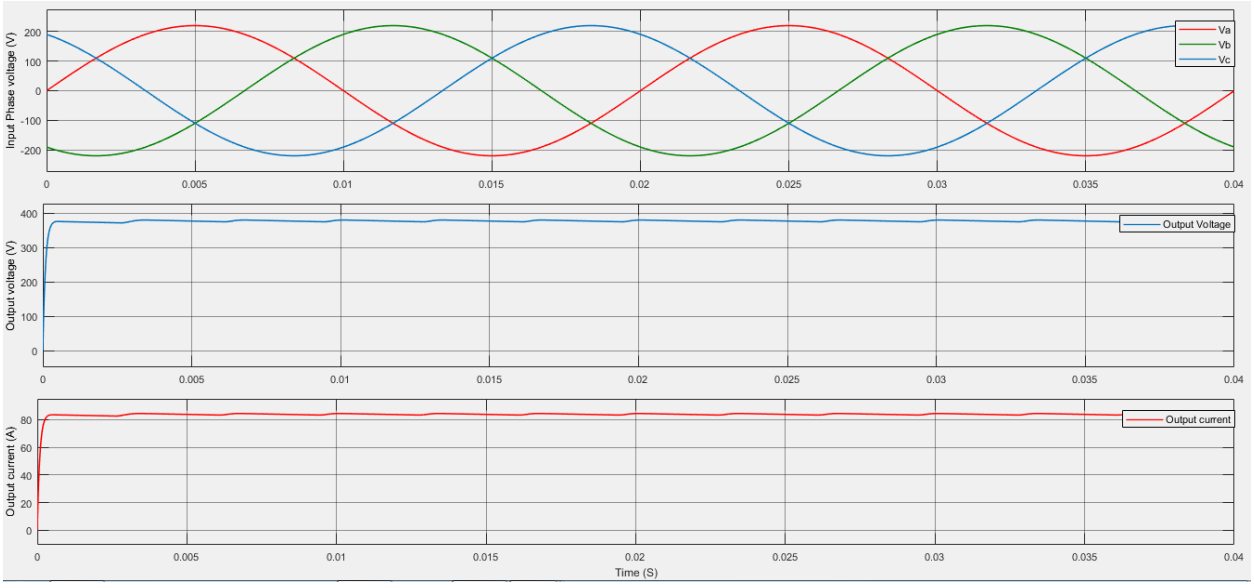

Figure 4. 2 Voltage and current waveforms of the three-phase bridge rectifier

Performance parameters of three phase full bridge diode rectifier

The Form Factor (*FF*) is the fraction of the rms value of the voltage output (V_L) to the value of average of the voltage output (V_{DC}) [30]:

$$FF = \frac{V_L}{V_{DC}} \tag{4.3}$$

This parameter is quite important since it is an index of the efficiency of the rectification process. Having assumed the load to be purely resistive, it is possible to define the currents as [30]:

$$I_{DC} = \frac{V_{DC}}{R_L} \tag{4.4}$$

$$I_L = \frac{V_L}{R_L} \tag{4.5}$$

The rectification ratio (η_r), also known as rectification efficiency, is expressed by [30]

$$\eta_r = \frac{P_{DC}}{P_L + P_D} \tag{4.6}$$

where

$$P_{DC} = V_{DC} . I_{DC} \tag{4.7}$$

$$P_L = V_L . I_L \tag{4.8}$$

$$P_D = R_D . I_L^{\,2} \tag{4.9}$$

In equation (4.9), P_D represents the losses in the rectifier (R_D is the equivalent resistance of the rectifier). By using equation (4.7 & 4.8) and equation (4.4 & 4.5), equation (4.6) can be written as follows:

$$\eta_r = \frac{V_{DC} . I_{DC}}{V_L . I_L + R_D . I_L^{\,2}} = \frac{V_{DC}^{\,2}}{V_L^{\,2}} \cdot \frac{1}{1 + (R_D / R_L)} \tag{4.10}$$

Ideal switches are assumed, with no losses, i.e, $R_D = 0$. Therefore

$$\eta_r = \left(\frac{V_{DC}}{V_L}\right)^2 = \left(\frac{1}{FF}\right)^2 \qquad 4.11$$

The Ripple Factor (*RF*) is another essential parameter used to explain the quality of the rectification. It shows the smoothness of waveform of the voltage at the output of the rectifier. The *RF* is defined as the fraction of the effective AC component of the load voltage versus the DC voltage:

$$RF = \frac{\sqrt{V_L^{\,2} - V_{DC}^{\,2}}}{V_{DC}} = \sqrt{FF^2 - 1} \qquad 4.12$$

Table 4.1 summarizes the main performance parameters for the three phase topologies described here [30].

Table 4. 1 Performance parameters for three phase bridge rectifier [30]

Performance parameters	**Three phase bridge rectifier**
Peak Repetitive reverse voltage V_{RMS}	$1.05 V_{DC}$
rms input voltage V_{Srms}	$0.428 V_{DC}$
Diode average current $I_{F(AV)}$	$0.333 I_{DC}$
Diode forward current I_{FRM}	$3.14 I_{F(AV)}$
Form factor *FF*	1.0009
Rectification ratio η_r	0.998
Ripple factor *RF*	0.042
Output ripple frequency f_R	$6 f_{mains}$

As we can see from both current and voltage expression of the rectifier output, there is no degree of freedom for control of either voltage or current. However, the DC bus needs to be maintained within a certain range for a grid connected topology because of the stability problem. Thus, a boost converter is needed for DC bus voltage control.

4.2 Boost converter

The boost converter is a switched-mode power converter which can produce a DC voltage output larger than the DC voltage input. It is widely used in much clean energy application like electric vehicle battery system, PV system and wind power system. An ideal switch boost converter circuit is shown figure 4.3 [29]:

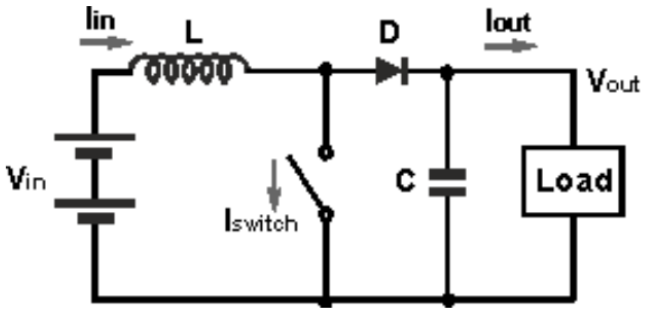

Figure 4. 3 DC-DC boost converter topology with ideal switch and diode [29].

A boost converter usually consists of the following components:

- DC input voltage Vin
- inductor L
- semi-conductor switch
- diode
- output capacitor and
- output load.

The input voltage provides the power to the whole circuit. By turning on and off of the switch, the output voltage will be larger than the input voltage because the inductor has to resist current change when the switch is turning on and off and produce a voltage. The output voltage must be boosted to 650 volts (around 2 time of grid line to line) higher than the grid line-line voltage. The circuit of both on and off mode of switch are shown in figure 4.4 and 4.5 [31].

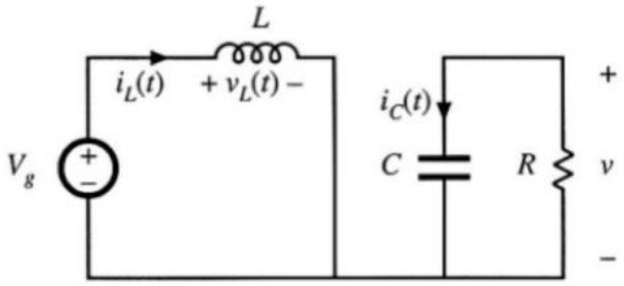

Figure 4. 4 Circuit of boost converter when the ideal switch is on [31].

The inductor is directly connected to the input voltage, and the capacitor and load resistor are isolated from the input. Ignoring the inductor resistor and capacitor resistor we can have:

$$V_L = V_g \tag{4.13}$$

$$i_c = -\frac{V}{R} \tag{4.14}$$

Where ***Vg*** is the input voltage, ***VL*** is the inductor voltage, ***ic*** is capacitor current, ***V*** is output voltage, and R is load resistor.

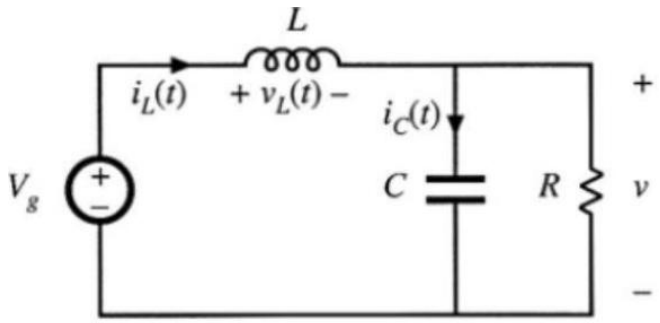

Figure 4. 5 Circuit of boost converter when switch is off [31]

When the switch is off, the circuit is a typical RLC circuit as shown in Figure 4.5. The current from DC input source now can flow to the load side. Now we have a new relationship of the voltage and current in this circuit:

$$V_L = V_g - V \tag{4.15}$$

$$i_c = i_L - \frac{V}{R} \tag{4.16}$$

Where $\boldsymbol{i_L}$ is the inductor current.

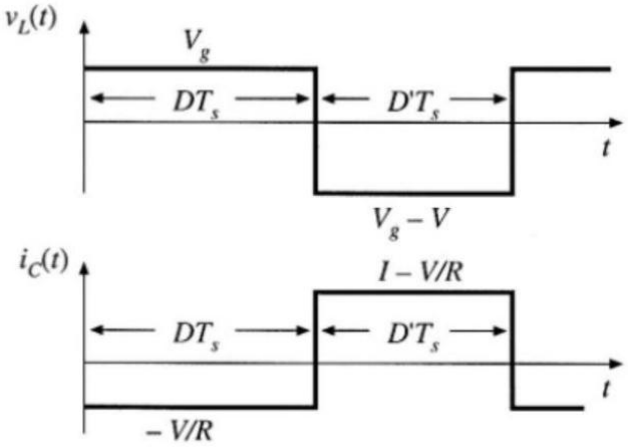

Figure 4. 6 Inductor voltage and capacitor current with a single switching cycle [31].

The inductor voltage and capacitor current waveform in a single switching period Ts are shown in figure 4.6. D is the duty cycle which is the portion of on during one cycle and D' is the portion of off in the same cycle. We all know that the inductor and capacitor do not consume energy during a complete switching cycle. Thus, the voltage-second applied on the inductor and current-second applied on the capacitor in each cycle must be zero. So, we have:

$$V_g DT_s + \left(V_g - V\right) D' T_s = 0 \tag{4.17}$$

$$-\frac{V}{R} DT_s + \left(I - \frac{V}{R}\right) D' T_s = 0 \tag{4.18}$$

The output voltage and current can be expressed as:

$$V = \frac{V_g}{D'} \tag{4.19}$$

$$I = \frac{V}{D' R} \tag{4.20}$$

Where: $D' = 1 - D$

From the equation, it is shown that with a constant dc voltage input, the output voltage can be amplified within a certain range by controlling the switching duty cycle. When the duty cycle is getting closed to 1, the inductor current will go to infinity based on the calculation. The large current will cause nonlinearity because of the practical inductor resistance and semiconductor forward

voltage. Power losses will increase, and the output voltage will drop dramatically. The ripple of the inductor current and capacitor voltage are important characters that need to be analyzed in boost converter circuit.

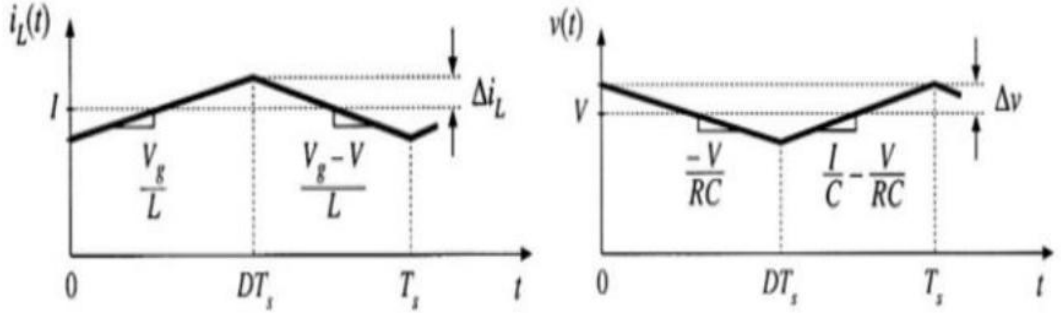

Figure 4. 7 Ripple current on the inductor and ripple voltage on the capacitor in one duty cycle.

The inductor current at the on mode is given by:

$$\frac{di_L}{dt} = \frac{V_L}{L} = \frac{V_g}{L} \qquad 4.21$$

From the current curve, we can see that the total change of current during this period is $2\Delta i_L$. Solving for Δi_L we have:

$$\Delta i_L = \frac{V_g}{2L} DT_s \qquad 4.22$$

The inductor current ripple is important because if the ripple current is too large and the calculated negative peak ripple crosses zero, the boost converter must run in discontinuous conduction mode (DCM). Under the DCM, we can no more apply the equation derived from the continuous conduction mode (CCM). To keep the converter running at CCM, there is a minimum inductance requirement depends on the circuits [31]:

$$L \geq \frac{V_{in(min)} * D}{2 * f_s * \Delta i_L} \qquad 4.23$$

where Δi_L is 20% to 40% of I_L

Assuming efficiency of boost converter is 1,

$$P = V_{in}.I_{in} = V_o.I_o \quad (4.24)$$

where $I_L = I_{in}$

$$I_L = \frac{P}{V_{in}} = \frac{29.94KW}{363.88V} = 82.28A$$

Taking 30%, $\Delta I_L = 0.3 * 82.28A = 24.68A$

$$I_o = \frac{29.94Kw}{650V} = 46.06A$$

$$L = \frac{V_{in(min)} * D}{2 * f_s * \Delta i_L} = \frac{363.88V * 0.44}{2 * 50KHz * 24.68A} = 64.9\mu H$$

Like the inductor current, the capacitor voltage at the on mode is:

$$\frac{dV_c}{dt} = \frac{i_c}{C} = \frac{V}{RC} \quad (4.25)$$

The voltage change on the capacitor during the on cycle is 2ΔVC. Solving for ΔVC we can derive:

$$\Delta V_c = \frac{V}{2RC} DT_s = \frac{I_o * D}{2 f_s * C} \quad (4.26)$$

The ripple voltage will directly be applied to the output load. The Large capacitor can eliminate the ripple voltage, but the size and cost will also increase. It is always a tradeoff selection between the capacitor size and maximum ripple voltage on the output [31].

$$C \geq \frac{I_o(max) * D}{2 f_s * \Delta V_c} \quad (4.27)$$

where ΔV_c is 1% to 5% of V_c, $V_c = V_o$

$$C = \frac{I_o * D}{2 f_s * \Delta V_c} = \frac{46.06A * 0.44}{2 * 50KHz * 0.01 * 650V} = 31.179\mu F$$

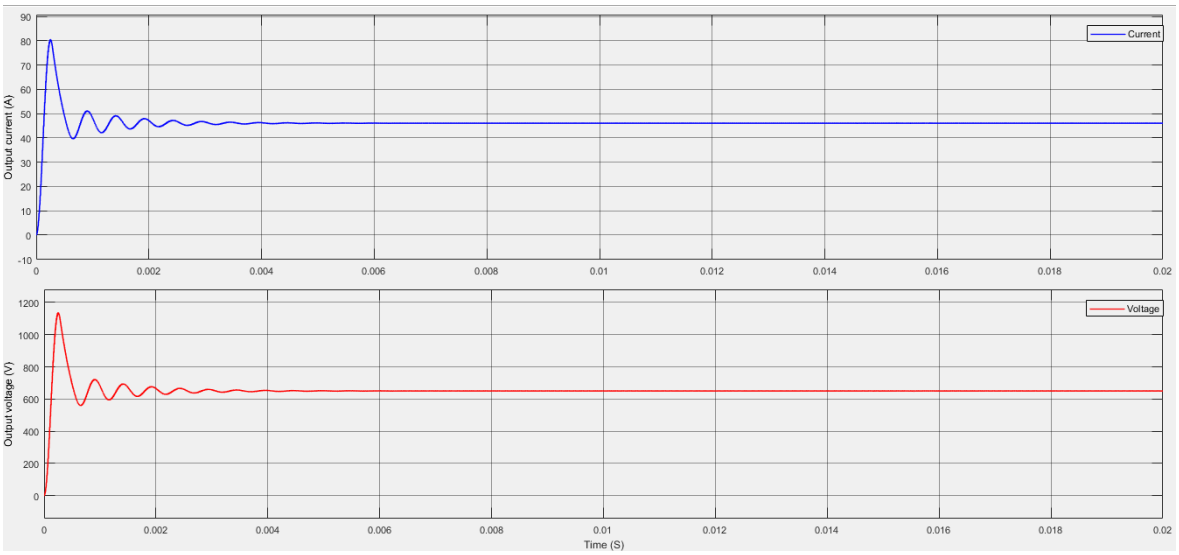

Figure 4. 8 DC boost converter output current and voltage wave form

4.3 Grid tie Inverter Design

Grid tie inverter plays a major role in many grid-connected distributed power generation systems because it is the converter that controls the quality of power transmitted to the grid. The synchronization with the utility grid is the main concern of the inverter control design because the grid frequency and voltage need to be regulated. If the inverter output cannot meet the local grid connection criteria, the power will not be allowed to deliver [32].

Voltage source inverter(VSI) and current source inverter(CSI) are the two types of inverter. The CSI use a DC current source as an input, and it is only usually used to drive high power AC motor. VSI is more commonly used in grid connection applications. The VSI is driven by a DC voltage source and can be more divided into two types: pulse width modulated inverter (PWM), and space vector modulated inverter (SVM) [32].

In this thesis, the Pulse-width Modulated inverter is used. PWM inverters take in a steady dc voltage. The inverter should conduct the magnitude and the frequency of ac output voltages, and the diode rectifiers are required to fix the line to line voltage. The inverter uses pulse-width modulation using it's switches, there are various methods for doing the pulse-width modulation in an inverter beneficial to frame the output ac voltages nearly similar to sine wave. The inverter only controls the frequency of the output where the input voltage controls the magnitude. The ac output voltage get a

waveform identical to a square wave to which the inverter got it's name. In inverters the power semiconductors devices always remains forward-biased due to the supply voltage, and therefore, self controlled forward device such as IGBTs and MOSFETs are suitable.

4.3.1 The three phase voltage source inverter

The 3-Φ voltage source inverter generates less harmonic distortion in the output voltage utilized in the phase to phase AC load. Also afford extra productive supply voltage related to sinusoidal modulation technique. The circuit model of three-phase voltage source PWM inverter is shown in Figure 4.9. The six power switches that form the output are T_{A+}, T_{A-} ;T_{B+},T_{B-}; to T_{C+},T_{C-} , which are controlled by the switching variables. while an upper transistor is switched on, the corresponding T_{A-} ,T_{B-},T_{C-} becomes 0. Therefore, the on and off states the upper transistors T_{A+}, T_{B+}, T_{C+}, can be used to regulate the output voltage. Each power switch can be on and off, On = 1, Off = 0 [33].

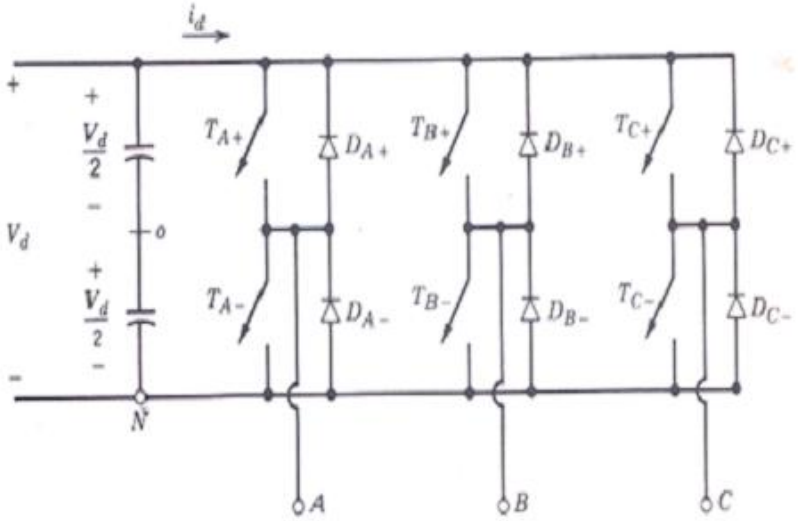

Figure 4. 9 Three phase inverter [33].

4.3.2 LC Filter

Output voltage wave is synchronized with the grid voltage. So the PWM inverter will inject ripple current in to the grid. The output LC filter is connected to remove high switching frequency components from output current of inverter [34]. The simulation design of LC filter is shown in figure 4.10. The filter is designed taking into account the following parameters for the grid and inverter as shown in table 4.2. The value of L is designed based on current ripple. Switching and conduction losses is smaller for small ripple. Usually the ripple current can be selected as 10% - 15%

of rated current. Considering 10% ripple at the rated current the designed value of inductor (L) in the system [35]-[36] is given by equation (4.28).

$$\Delta i_{Lmax} = \frac{V_{dc}}{8*L*f_s} \qquad 4.28$$

The capacitor C is designed based on reactive power supplied by the capacitor at fundamental frequency. In this design reactive power can be chosen as 15% of the rated power is given by equation (4.29) [35].

$$C = \frac{15\% * Prated}{3*2\pi f*V^2 rated} \qquad 4.29$$

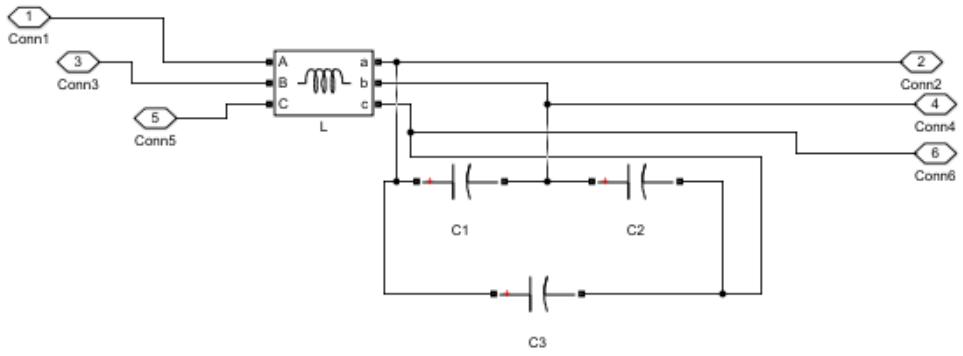

Figure 4. 10 LC filter

Table 4. 2 design parameters for LC filter

Line Voltage	Vab L-L =380 V
DC source voltage	Vdc = 650 V
Modulation index	1
Nominal frequency	50 Hz

To simulate the active and reactive power that flows in to the grid, the power expression in the d-q synchronous frame is given as:

$$P = \frac{3}{2}(V_d i_d + V_q i_q) \qquad 4.30$$

$$Q = \frac{3}{2}(V_q i_d - V_d i_q) \qquad 4.31$$

Where V_d and V_q are the inverter voltage in d-q synchronous edge and i_d and i_q are the inverter

current in the d-q synchronous edge. If the d-q frame is selected randomly, there will be coupling problem because of the cross product of the d axis component and q axis component. Such a coupling will bring difficulty in inverter control and deteriorate the output power quality and the efficiency. Instead of an arbitrary d-q synchronous frame, the q axis is forced to align the phase *a* space vector and rotate at the synchronous speed. The d-axis voltage become zero by this synchronization.

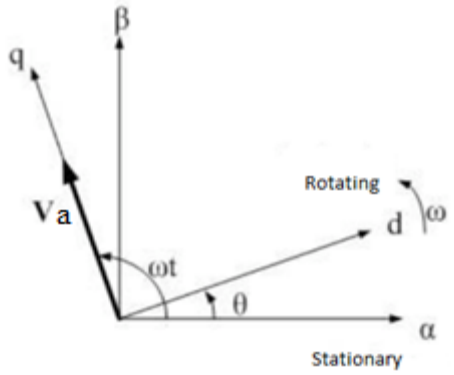

Figure 4. 11 α-β frame and rotational d-q frame decomposition with grid frequency ω and a random phase angle θ [13].

As shown in figure 4.11, phase *a* voltage does not have decomposition on d axis because q axis is aligned with it. Therefore, we have:

$$V_q = V \tag{4.32}$$

$$V_d = 0 \tag{4.33}$$

by substituting equation (4.32 and 4.33) in to equation (4.30 and 4.31) , it gives:

$$P = \frac{3}{2}(V_q i_q) \tag{4.34}$$

$$Q = \frac{3}{2}(V_q i_d) \tag{4.35}$$

Considering the inverter loss, active power can be expressed as:

$$P=\frac{3}{2}(V_q i_q)=0.94V_{dc}i_{dc} \tag{4.36}$$

4.4 PLL design

Since the PLL to be developed will be working in a sampled system there is need to take into account the delay effect. The transfer function (TF) for the plant in figure 2.4 is just a lag and an integrating element [37].

$$G_P=\left(\frac{1}{1+sT}\right)\left(\frac{1}{s}\right) \tag{4.37}$$

The open-loop TF for the system in figure 2.4 is described as follows [37].

$$G_{ol}=\left(Kp\frac{1+s\tau}{s\tau}\right)\left(\frac{1}{1+sT}\right)\left(\frac{V_m}{s}\right) \tag{4.38}$$

The integrating element in the plant correspond to the following differential equation

$$G(S)=\frac{F(S)}{E(S)}=\frac{1}{S}\Leftrightarrow\frac{df}{dt}=e(t) \tag{4.39}$$

Which has to be solved numerically using Euler forward [37], and taking the Z-transform gives

$$s=\frac{Z-1}{T_S} \tag{4.40}$$

Using equation (4.40) the PI-regulator in the z-domain is shown as follows

$$G_{pi}=Kp\frac{1+s\tau}{s\tau}=Kp\frac{Z-1+\frac{T_S}{\tau}}{Z-1} \tag{4.41}$$

Rewriting the TF for the PLL system in equation (4.38) yields

$$G_{ol}=\left(K_P\frac{1+s\tau}{s\tau}\right)\left(\frac{1}{1+sT_S}\right)\left(\frac{V_m}{s}\right)=\frac{K_pV_m}{T_S}\frac{\left(s+\frac{1}{\tau}\right)}{s^2\left(s+\frac{1}{T_S}\right)}=\frac{K_pV_m}{aT_S}\frac{\left(as+\frac{a}{\tau}\right)}{s^2\left(s+\frac{1}{T_S}\right)} \tag{4.42}$$

Where;

G_p : transfer function of the entire system,

$(\frac{1}{1+ST})$: the system lag term,

T : Sampling period in seconds,

$(\frac{1}{S})$: Integrating element,

G_{ol} : Transfer function of open loop

V_m : Amplitude voltage level in volt and

K_p : Regulator gain

The 2nd order transfer function of a dynamic system is written as [37];

$$F = \frac{\omega_o{}^2(Ks+\omega_o)}{s^2(s+K\omega_o)} \qquad 4.43$$

where *a* represent normalization factor and ωc is the crossover frequency which has the value of the grid and inverter output frequency. Comparing equation (4.42) and (4.43) gives the following identifications.

$$\begin{cases} \omega_c = \dfrac{1}{aT_s} \\ \tau = a^2 T_s \\ K_p = \dfrac{1}{aV_m T_s} \end{cases} \qquad 4.44$$

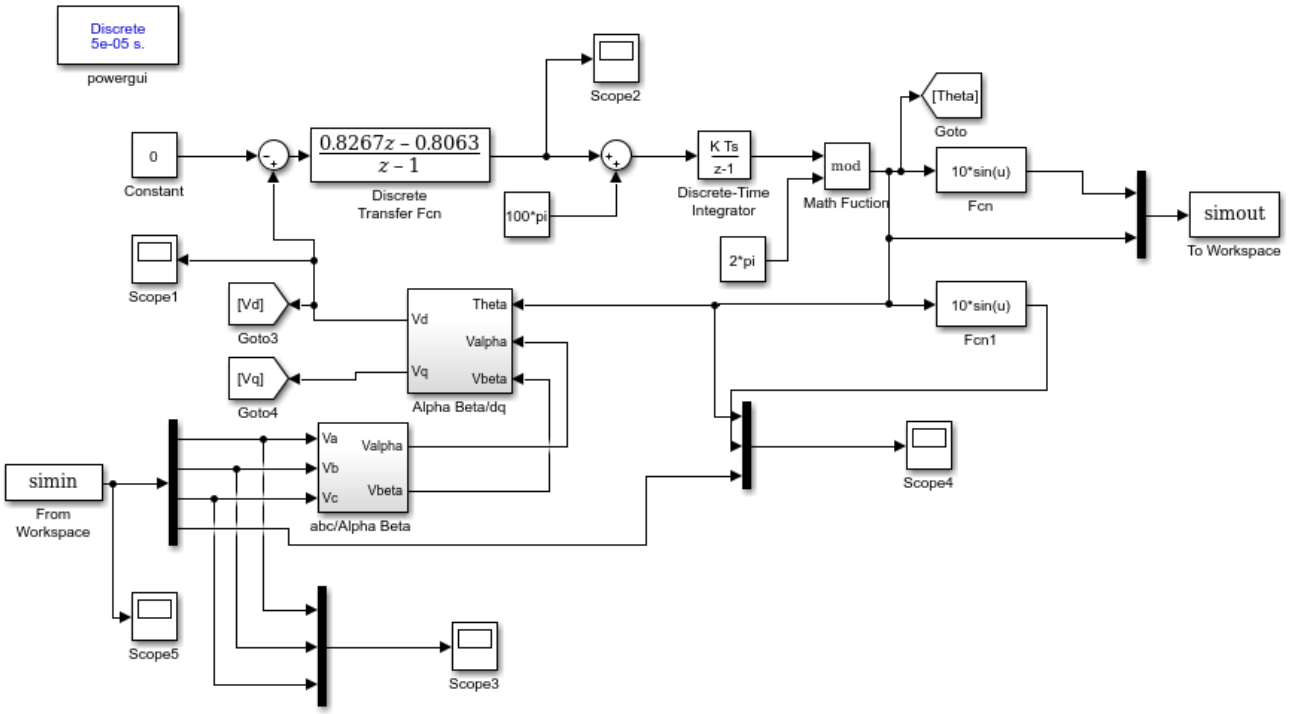

Figure 4. 12 The Simulink Simulation Setup of the Phase Lock Loop System. The box named Discrete Transfer Fcn is the PI-regulator.

From simin in figure 4.12, four signals are imported. The fourth signal is a scaled version of input signal Va and makes it easier to plot the phase angle output and the reference signal together. The boxes named abc/ α-β and α-β /dq in are the implementation of the transformation matrices in equation (2.5) and (2.7) respectively. The details of these sub systems are given in figure 4.13.

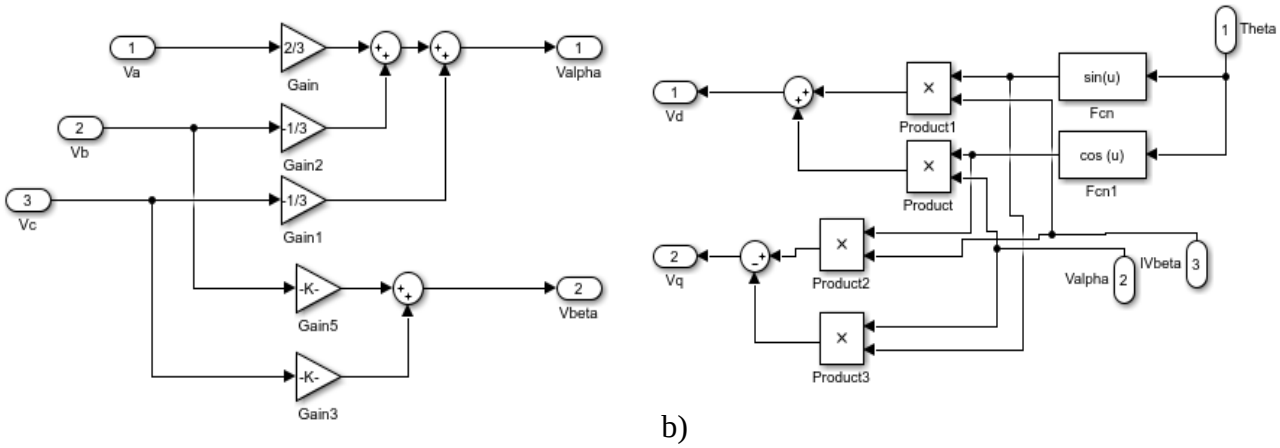

Figure 4. 13 a) Transformation from abc to α-β. Gain 5 is - $\sqrt{3}$ /3 and gain 3 is $\sqrt{3}$ /3. b) Transformation from α-β to dq.

System Characteristics

The inverter grid voltage is 380V which is the value of the line-to-line voltage at the point of grid connection. Hence, *Vm* = 380V, *Ts* = 1/2000s = 0.5ms, choosing crossover frequency 50Hz and substituting the parameters for *Vm* and *Ts* in equation (4.37) gives

$$\begin{cases} a = 6.3662 \\ \tau = 0.0203 \\ K_p = 0.8267 \end{cases} \qquad 4.38$$

Simulation of PLL with Design Gains

With the PLL parameters set as $a = 6.3662$, $\tau = 0.0203$, $K_p = 0.8267$, $V_m = 380V$, $T_s = \frac{1}{2000}s = 0.5ms$ and choosing crossover frequency 50Hz, the transfer function of the PI regulator in equation (4.35) becomes

$$G_{pi} = K_p \frac{z - 1 + \frac{T_s}{\tau}}{z - 1} = \frac{0.8267z - 0.8063}{z - 1} \qquad 4.39$$

The complete model description of the system with the PI regulator in MATLAB Simulink environment is implemented and shown in figure 4.12. Based on the design, the PLL is developed for grid voltage of 380V and simulation of the entire system is done in Simulink.

Vabc is the sensed grid voltage which is transformed in to DC components using coordinate transformation *abc-dq* and the PLL gets locked by setting Vd* represented by the constant block to zero. The loop filter PI is a low pass filter represented by the Discrete-Transfer Function block. It is used to suppress high frequency component and provide DC controlled signal to voltage controlled oscillator (VCO) which acts as an integrator represented by the Discrete-Time Integrator block. The output of the PI controller is the inverter output frequency that is integrated to obtain inverter phase angle θ. When the difference between grid phase angle and inverter phase angle is reduced to zero PLL becomes active which results in synchronously rotating voltages *Vd* = 0 and *Vq* gives magnitude of grid voltage.

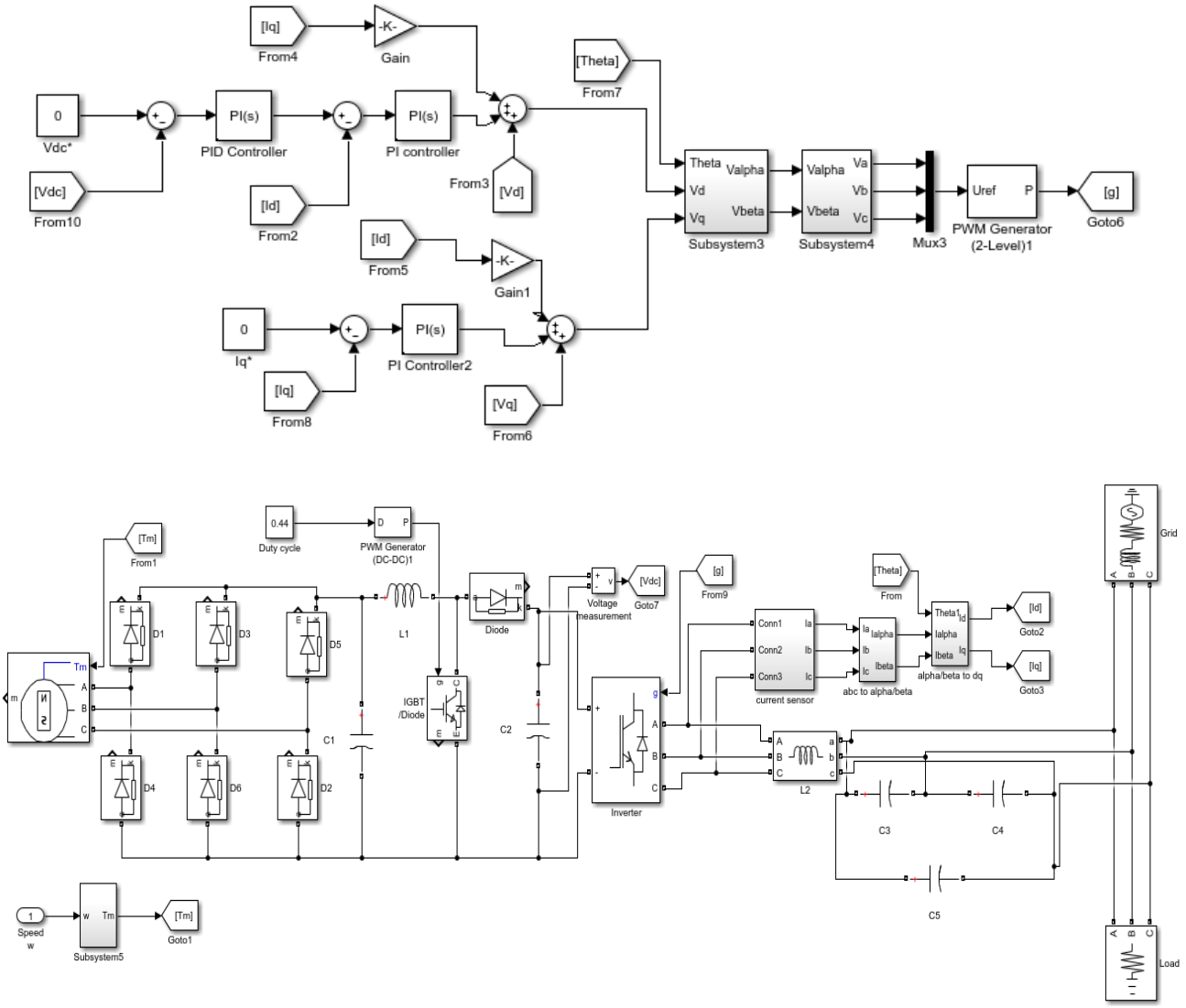

Figure 4. 14 Over all block diagram implemented in simulink

CHAPTER FIVE

SIMULATION RESULTS AND DISCUSSIONS

5.1 Introduction

This chapter presents a simulation conducted and results obtained from the grid connected micro hydropower plant using Matlab Simulink for different grid conditions. The Simulink model shown in figure 4.12, 4.14 and the code written in Appendix A are used to carry out simulation studies and analyses the performance of phase locked loop under different operating conditions.

5.2 Simulation Results

The response of the system is tested for ideal and non-ideal grid conditions.

5.2.1 Simulation for ideal grid conditions

The system performance is studied under an ideal condition when the line-to-line voltage is 380V and the frequency of the inverter and grid are set at 50Hz. The three-phase voltages for the grid and the inverter output are shown in figures 5.1 (a) and (b) respectively. Figure (5.1a) is the output voltage from the utility grid while figure (5.1b) is the output voltage of the micro hydro power whose frequency and phase are supposed to be matched to that of the running network.

For simulation, the required three phase voltage signals with controllable magnitude, phase and frequency as specified by the grid has been generated by writing their respective scripts in Matlab and imported using the Simin block. Based on the simulation, the output of PLL is in synchronism with grid as shown in figure 5.2. It can be observed that the PLL tie the grid and inverter phase voltages together, enabling them to operate in unity. The blue line comes from the inverter and the pink line comes from the grid.

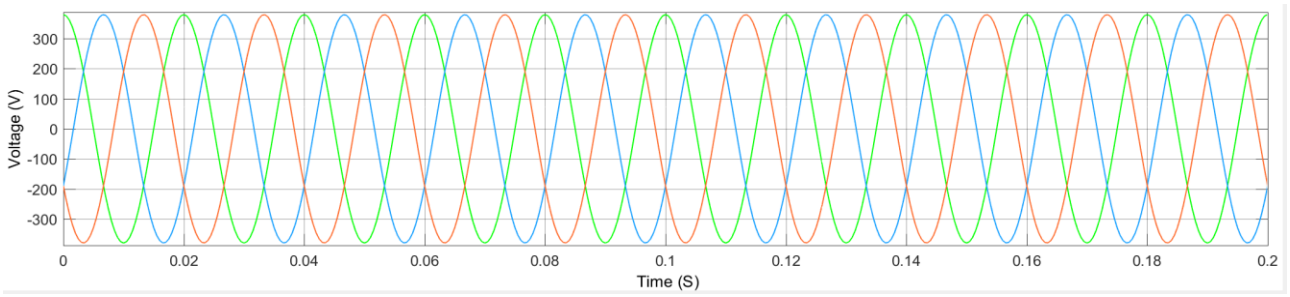

a)

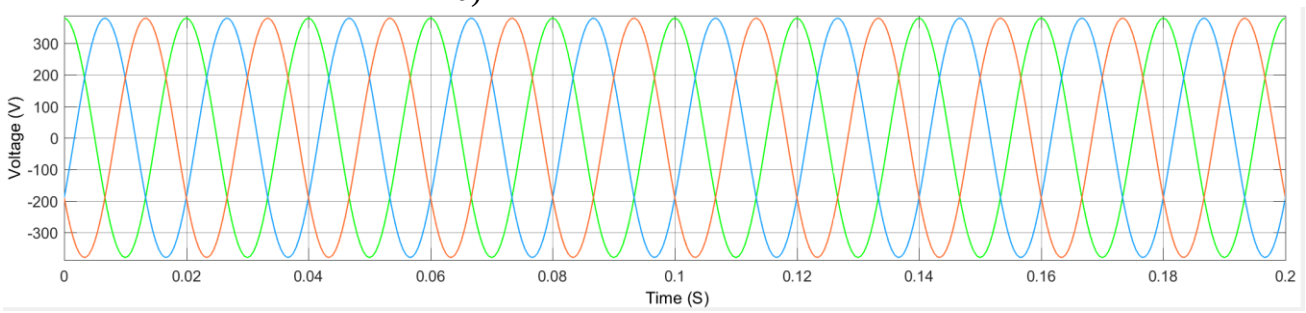

b)

Figure 5. 1 Output Waveforms of (a) Grid (b) inverter Voltages

The ideal and sampled sine signals are created in MATLAB, see Appendix A for code. Output of PLL is presented in figure 5.2 shown below.

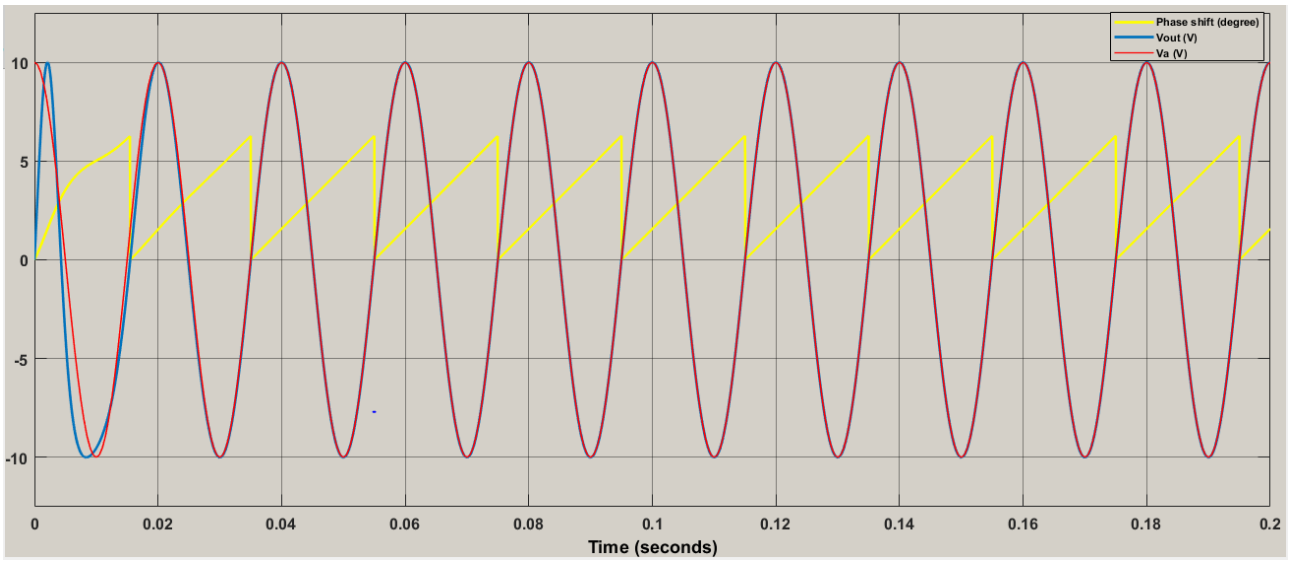

Figure 5. 2 PLL output with ideal grid conditions. From the phase angle (yellow) a sine wave is created (blue) and locks on to the scaled reference signal Va (pink).

The output of the PI-regulator is observed for this ideal grid condition, as shown in figure 5.3. This output can be thought of as a step response of the system.

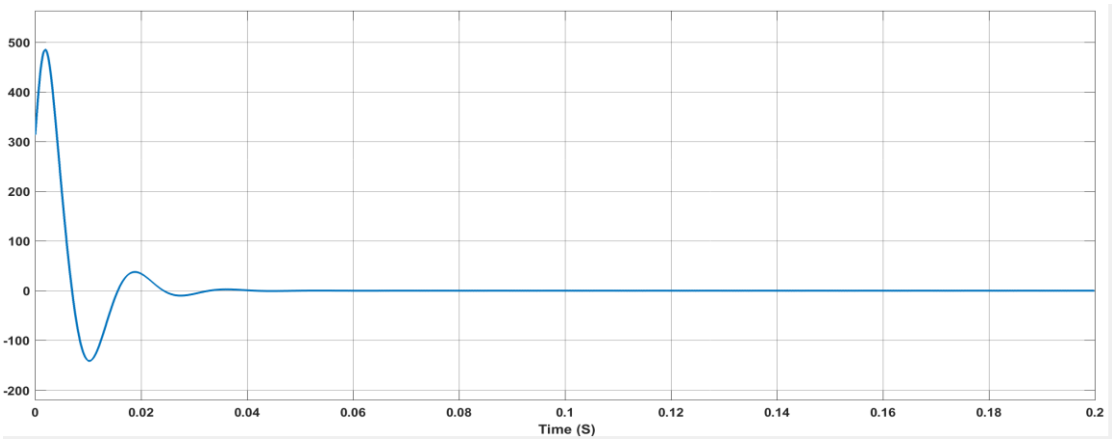

Figure 5. 3 Output of PI-regulator, this can be thought of as a step response for the system.

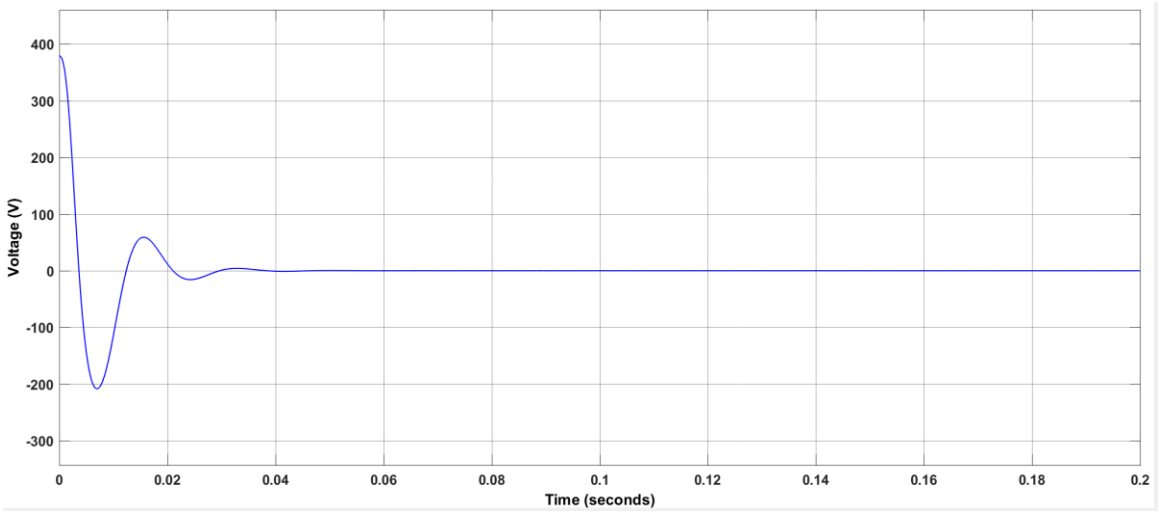

Figure 5. 4 Vd output while the voltage space vector is synchronized with the q-axis.

The PLL system with the PI-regulator gains from equation (4.38) is able to track the phase satisfactory when the grid conditions are ideal and no changes will be made in the gains.

5.2.2 Simulation for non-ideal grid conditions

The response of the grid to certain perturbations and the ability of the PLL to accommodate this disturbances were described as follows.

Amplitude variation

Voltage sags or swells occur when large loads are suddenly connected to or disconnected from the grid respectively. In this work, a sudden drop of voltage magnitude by 10% in all three phases was applied. The output when voltage sag happen is shown in Figure 5.5.

It can be observed that, the amplitude is varied after two periods, the amplitude decreased by 0.1 of the original value which indicates a voltage sag. The resulting PLL output in response to this sag is presented in figure 5.6.

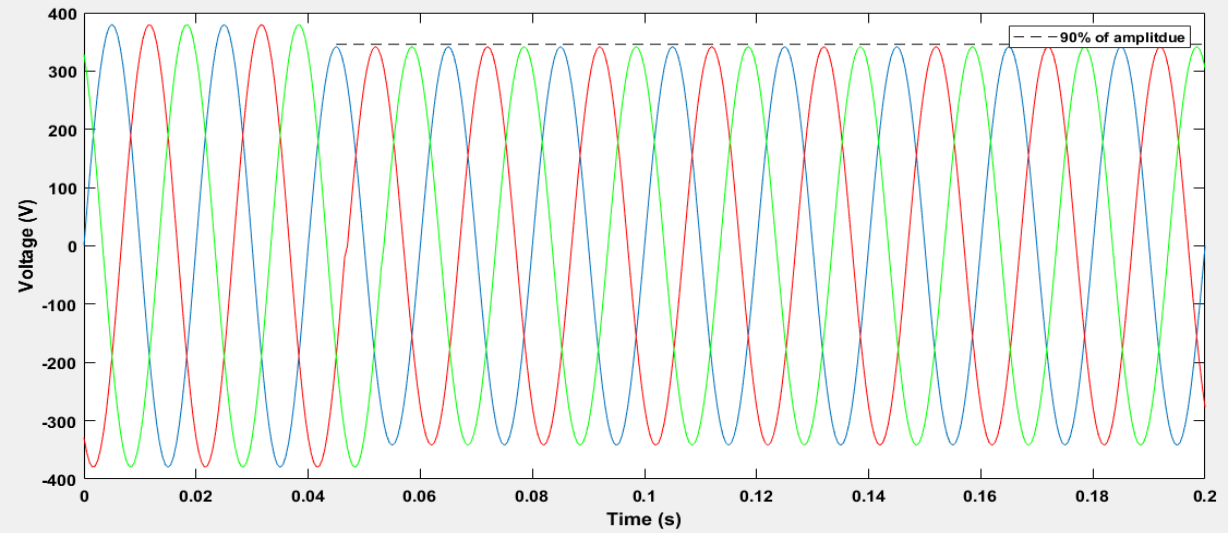

Figure 5. 5 Input signals with amplitude decreasing to 90% of the original value

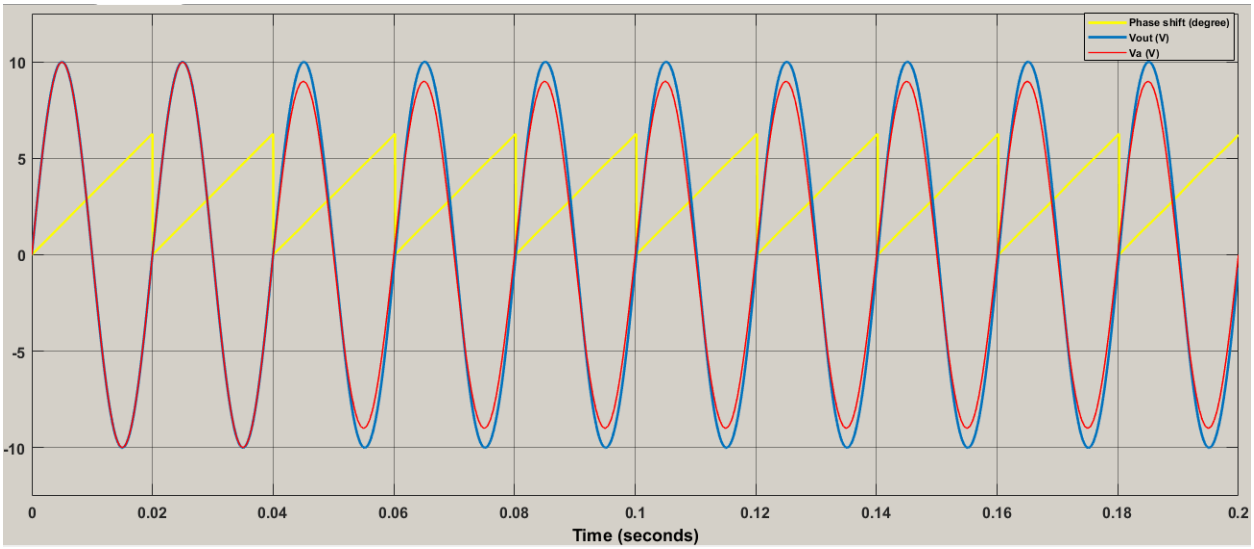

Figure 5. 6 PLL output for input with decreased amplitude

It is shown that with the PLL already phase locked with the system, there was no change in d axis voltage and the q axis voltage accurately tracks the system voltage magnitude. So no disturbance was observed in phase tracking.

Frequency variation

The PLL system was tested for input signals with frequency 55Hz as shown in figure 5.7.

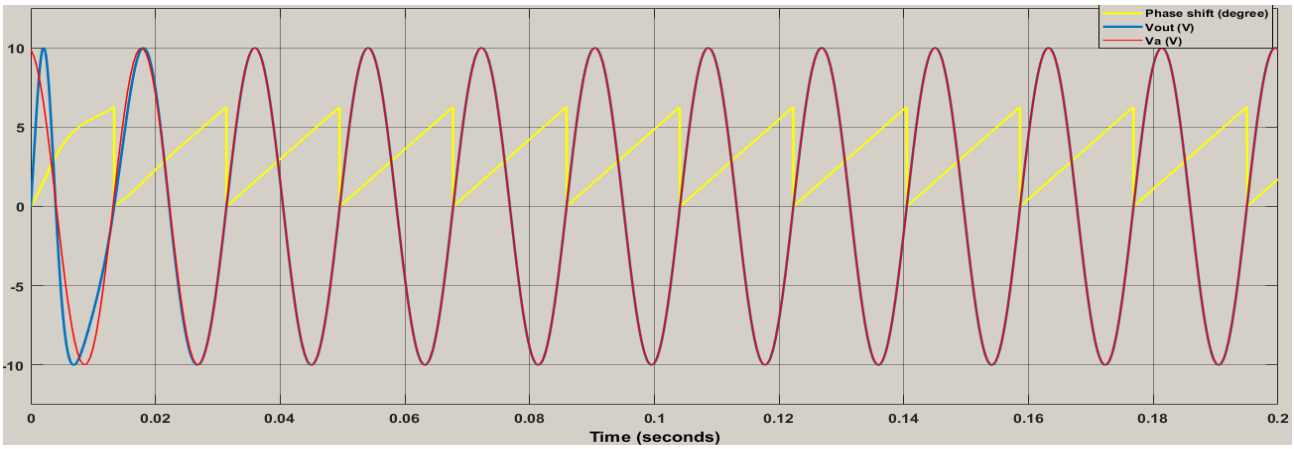

Figure 5. 7 PLL output for grid with frequency 55Hz.

In figure 5.8 the PI-regulator output is shown. Now the PI-regulator output is supposed to approach 2* π*5 = 31.4159 instead of 0 as for the ideal input signals.

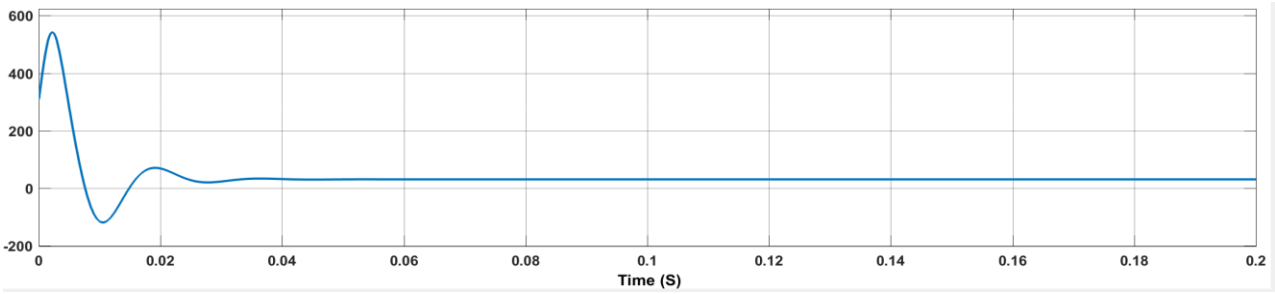

Figure 5. 8 PI-regulator output of input signals with 55Hz frequency leads to a PI-regulator output of 31.4.

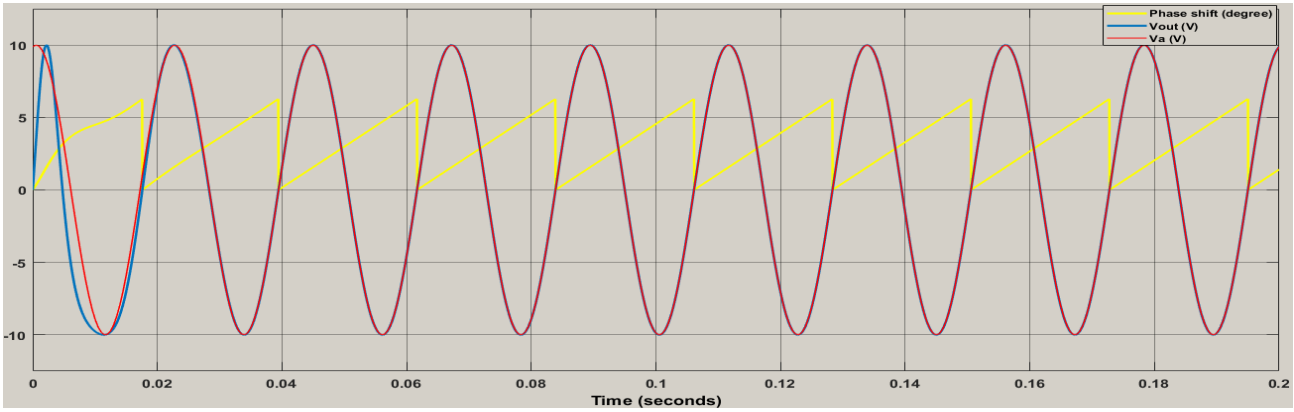

Figure 5. 9 PLL output for grid with frequency 45Hz.

In figure 5.10 the PI-regulator output approaches 2* π*(-5) = -31.4159 instead of 0 as for the ideal

input signals.

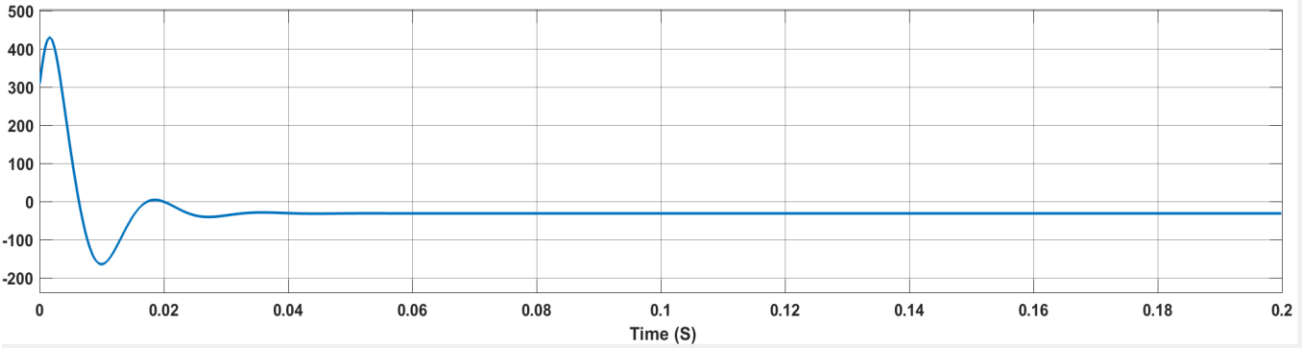

Figure 5. 10 PI-regulator output of input signals with 45Hz frequency leads to a PI-regulator output of -31.4.

Phase jump

Sudden phase change in load terminal voltage may occur if a large load is withdrawn from the supply system or due to faults in the grid. It is observed that the input signals making a phase jump was simultaneously applied to all three phases as shown in figure 5.11.

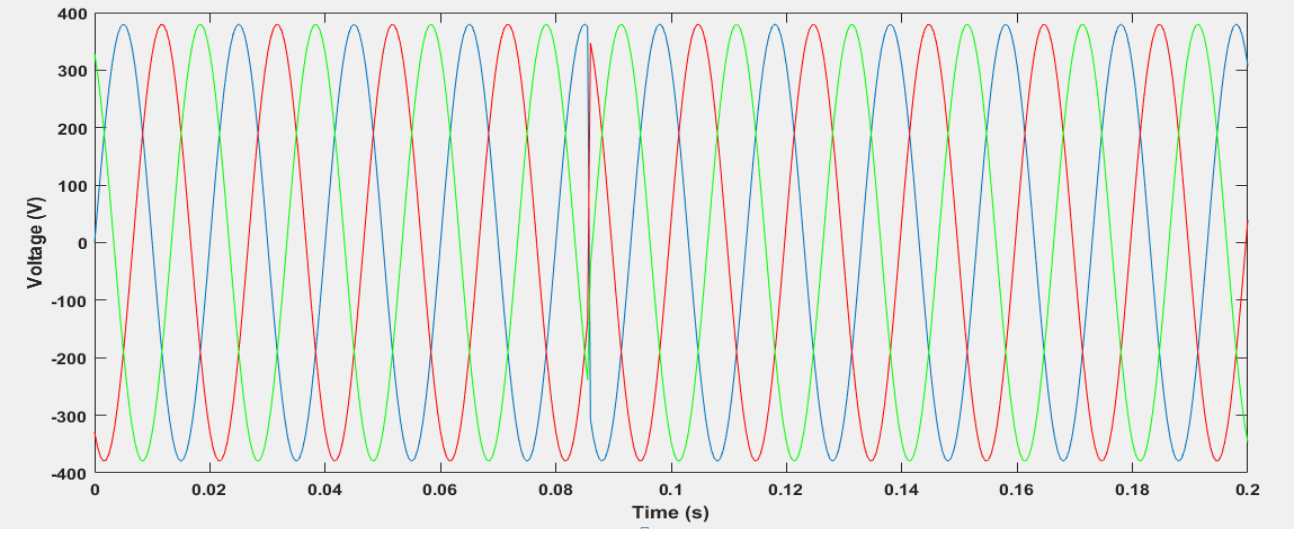

Figure 5. 11 Input Voltage with Phase Jump

The PLL output for input signals making a phase jump simultaneously in all three phases is shown in figure 5.12.

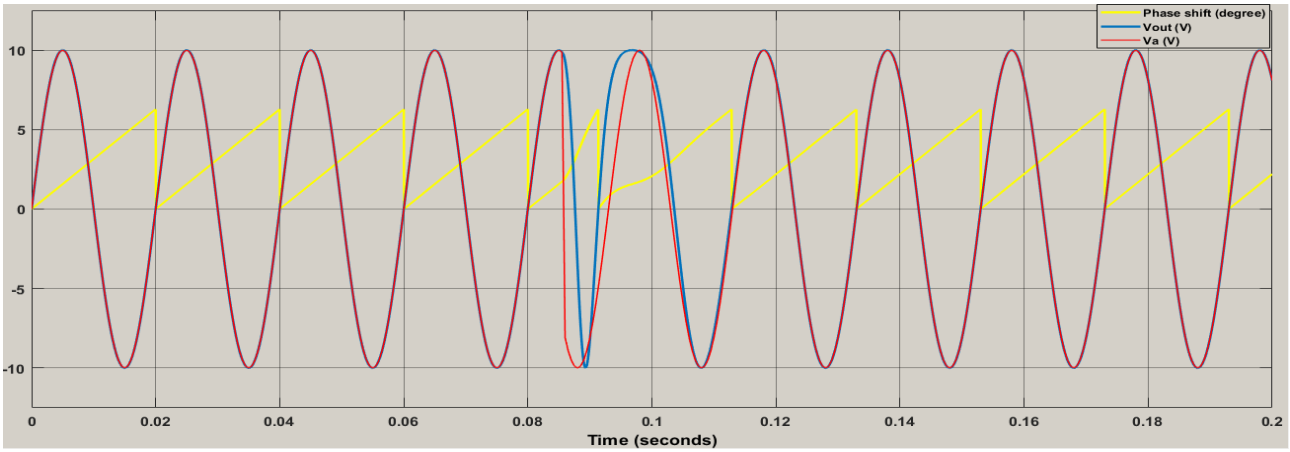

Figure 5. 12 PLL Output for Input Signals with Phase Jump.

Three phase voltage unbalance

The performance of the PLL system when subjected to an input signals with voltage unbalances between the three phases i.e., an amplitude of Vb is 0.85*V, that of Vc is 1.15*V while that of Va is unchanged was analyzed as highlighted in figure 5.13 and the response of the system obtained is shown in figure 5.14

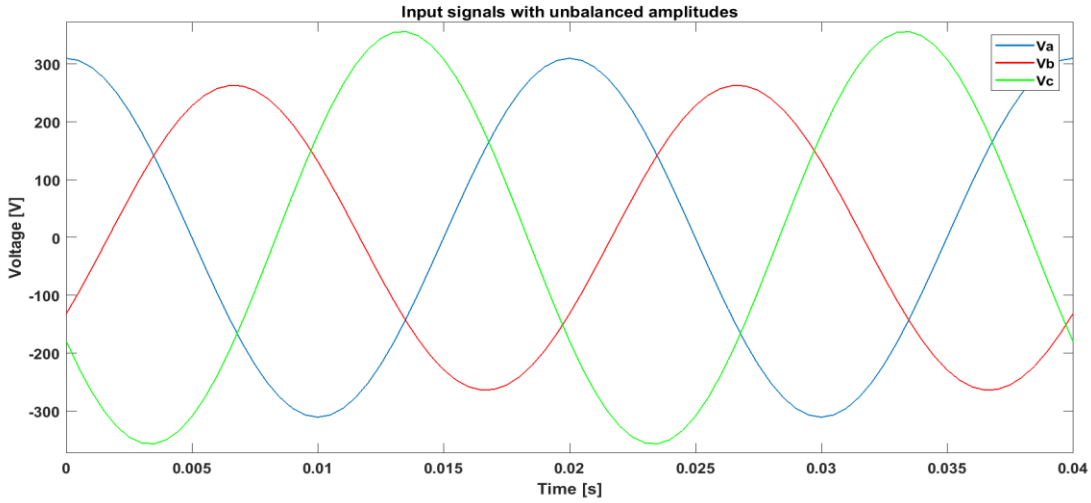

Figure 5. 13 Three-Phase Unbalanced Voltages Input.

The system was able to synchronize the grid and the micro hydropower system, in less than around 0.02Sec, as shown in figure 5.14.

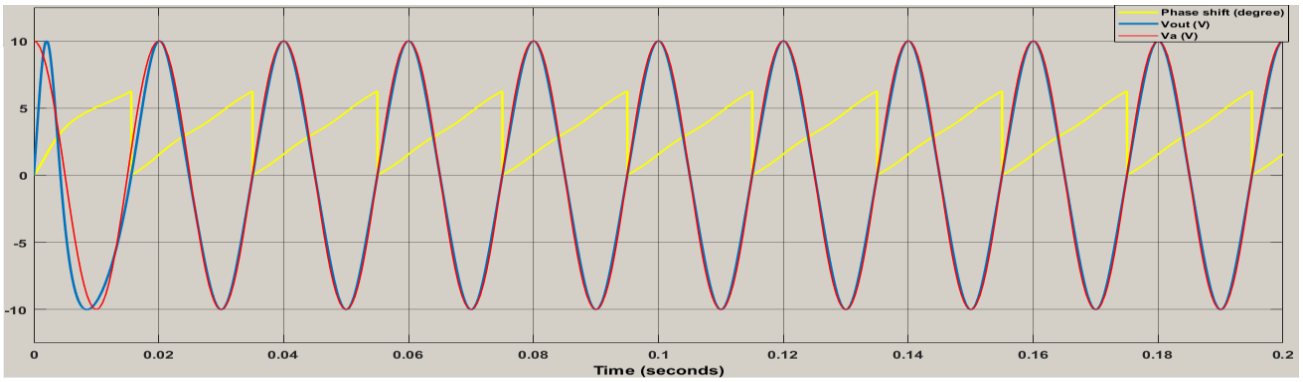

Figure 5. 14 PLL Output for Input Signals with Unbalanced Voltages.

The PI regulator output response to this disturbances is taken and presented in figure 5.15.

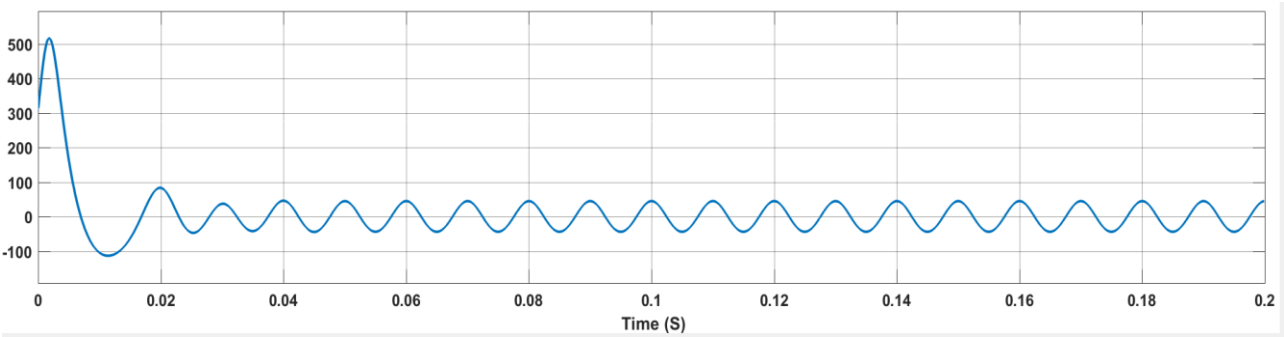

Figure 5. 15 PI-Regulator Output with Three Phase Voltage Unbalance Input Signal.

The PI regulator changes to an impulse response within around 0.02Sec, and attained an oscillatory state when subjected to voltage unbalance. Thus, leading to an inaccurate phase tracking.

Three phase unbalanced phase shifts

The performance of the system for the input signals that have not the proper phase shift of 120° relative to each other i.e., phase shift of -130° and -230° for phase b and c respectively is shown figure 5.16.

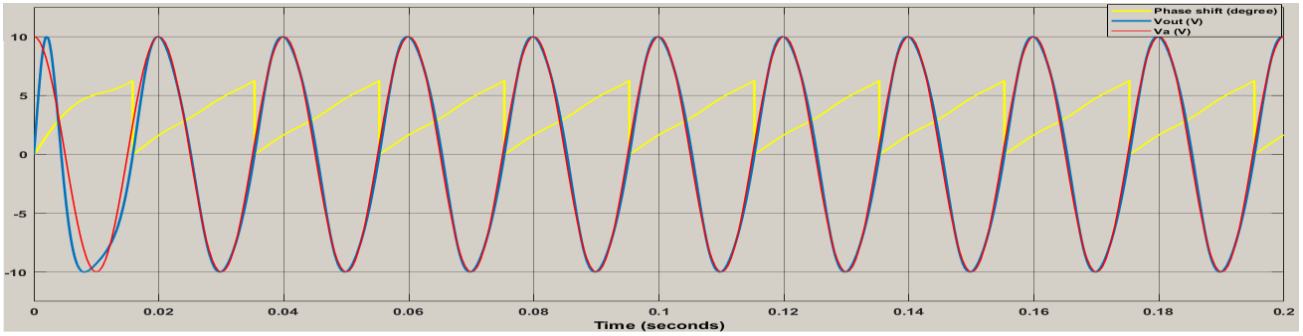

Figure 5. 16 PLL output for input signals with improper phase shifts

The PI regulator changes to an impulse response for three phase unbalanced phase shifts is shown in figure 5.17

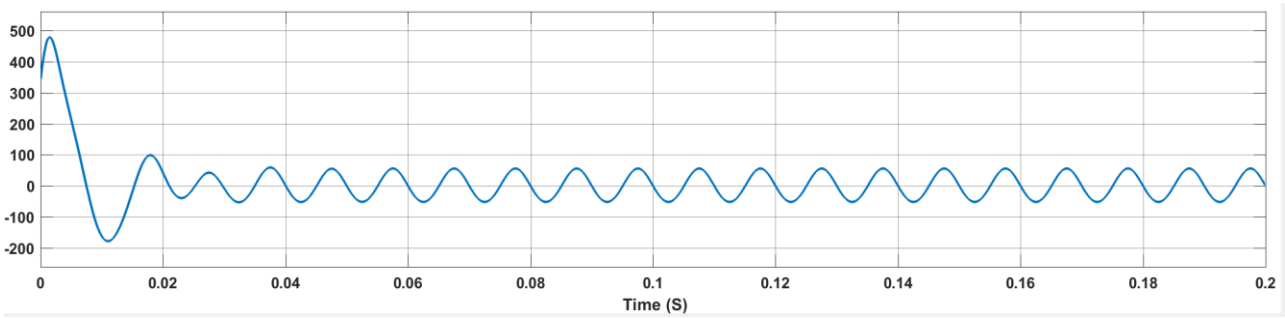

Figure 5. 17 The PI-regulator with input signals with improper phase shifts

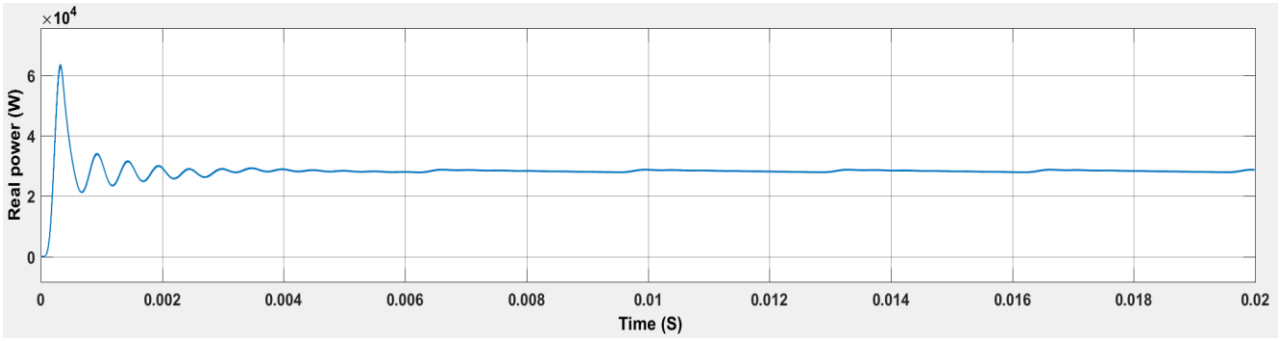

Figure 5. 18 Active power that flows in to the grid

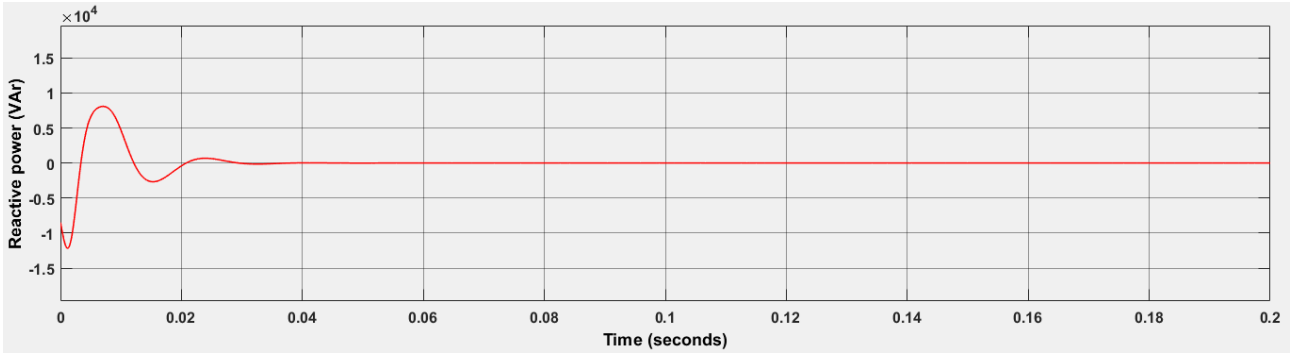

Figure 5. 19 Reactive power that flows in to the grid

5.3 Discussions

The objective of performed analysis on the designed power electronics and PLL were to connect micro hydro power to the utility network and analyze their performance for different conditions of grid. In this research PLL system together with the PI-regulator gain perform well for ideal grid condition synchronization with the output of the inverter. The system characteristics has been analyzed in MATLAB and showed the expected behavior. For ideal grid conditions the phase angle was tracked and relatively fast (synchronized almost after 0.015 seconds) and precise.

Different non-ideal grid conditions were simulated and almost all were handled well by the system. When amplitude was decreased to 90%, the system can track the phase angle but less precise, still within an acceptable range. Since the phase angle and frequency of the input signal is independent of amplitude, it is surprising that the output of the system is also independent of the amplitude. Voltage variations of more than this magnitude is not a part of normal operation; but it can be considered in cases of more severe faults when the grid collapse results in major voltage variation.

Also the system could easily track the phase when the frequency was shifted from 50Hz to 55Hz or 45Hz. In a real grid, frequency variations are in smaller magnitude relatively. The only difference from the ideal case is that the PI-regulator now approaches $2\pi*5$ rad/s for 55 Hz and $-2\pi*5$ rad/s for 45Hz instead of zero. On the other hand, for the phase jump that was simultaneously applied to all three phases, the phase angle was tracked with in around 0.02 seconds. Unbalances in the three phase input signals were overall handled by the system. For voltage unbalances and improper phase shift the phase angle was tracked but with less accuracy compared to the ideal case and also, the PI regulator changes to an impulse response within around 0.02Sec, and attained an oscillatory state. Thus, leading to an inaccurate phase tracking.

Finally, the real power delivered to the grid has higher overshoot before reaching the steady state level, because it is connected to the full load of the grid. The reactive power becomes zero after some oscillation (at around 0.03 seconds) because Id is maintained as zero.

CHAPTER SIX

CONCLUSIONS, RECOMMENDATIONS AND FUTURE WORK

6.1 Conclusions

In our country several MHPP are off-grid mode, where many of them are shut down due to grid connection challenges and the rest are suffering the same problem because of the expansion of the grid to those area. So, this thesis was aimed to develop a simple and cost effective solution to connect those available MHP to the grid. Power converters and PLL are developed to study the connection challenges of micro hydropower to the grid. Power converters improved the power quality that is delivered to the grid by minimizing the harmonics produced, providing a better ride through capability of the power generation, providing reactive power control or voltage regulation at the distribution system connection point. Also for synchronization PLL is designed in order to track the phase angle of the grid and it has been successfully achieved.

A mathematical model and design that represents the complete micro hydropower system including generator, turbine and power converters were developed for the Huluka river optimal micro hydro sizing ($0.244m^3/s$). Also, the modeled turbine and generator can operate at the flow rates of $0.094m^3/s$ and $0.103m^3/s$. However, at these flow rates turbine and generator were inefficient because they operate under their capacity.

The performance of the proposed system was tested through simulation using Matlab/Simulink. It was observed from the simulation results that the PI-regulator gains Kp = 0.8267 and τ = 0.0203 were calculated and for ideal grid conditions, with amplitude Vm = 380V and frequency f = 50Hz, the phase angle was tracked fast and accurate. The system was also simulated for several non-ideal grid conditions. Variations in amplitude, variation in frequency, Phase jumps and three phase voltage unbalance were handled well by the system.

In conclusion, connecting MHP to the grid through power converters and PLL is the promising method and considering the overall efficiency of the system(0.938), 28.14KW power has been delivered to the grid.

5.2 Recommendations and Future Work

In this thesis, the power converters and PLL are tested only for MHP system. However, their performance can be investigated for synchronizing distributed energy sources and other renewable technologies. Moreover, prototype of the system can be implemented and tested with grid voltages as input signal. Also, more conditions such as flicker, dip and notch should be made for better performance analysis. In addition, the cost benefit of micro hydropower plant for huluka river can be analyzed in detail.

REFERENCES

[1] EPA (Environmental Protection Authority), The Conservation Strategy of Ethiopia Volume I: The Resources Base, Its Utilisation and Planning for Sustainability, Addis Ababa, 1997a.

[2] I. Salhi, S. Doubabi, "Fuzzy Controller for Frequency Regulation and Water Energy Save on Micro-Hydro Electrical Power Plants," International Renewable Energy Congress, Tunisia, November 2009.

[3]Ethiopian Energy Situation. Retrieved 2018, EEPCo, from https://energypedia.info/wiki/Ethiopia-Energy-Situation.

[4] Micro hydropower Systems. (n.d.). Retrieved November 11, 2018, from https://energy.gov/energysaver/buying-and-making-electricity/microhydropower-systems.

[5] Ensuring the Sustainability of Rural Electrification in Nepal. (n.d.). Retrieved December 20, 2018,fromhttp://www.worldbank.org/en/news/feature/2015/09/26/ensuring-sustainable-rural-electrificationin-nepal

[6] About Micro grids. (n.d.). Retrieved April 11, 2017, from https://building microgrid.lbl.gov/about microgrids

[7] Microhydropower Systems.(n.d.). Retrieved November 11, 2019, from https://energy.gov/energysaver/buying-and-making-electricity/microhydropower-systems

[8] Planning a Micro hydropower System. (n.d.). Retrieved March 11, 2019, from https://energy.gov/energysaver/planning-microhydropower-system

[9] Bedi, E. (n.d.). DIERET: Hydro. Retrieved April 03, 2019, from http://www.inforse.org/europe/dieret/Hydro/hydro.html

[10] A. E. Fitgerald, J. C. Kingsley, and S. D. Umans, Electric Machinery. New York: McGraw-Hill, 1990.

[11] Jim Doucet, Dan Eggleston, and Jeremy Shaw, DC/AC Pure Sine Wave Inverter, NECAMSID, MQP Term A-B-C 2006-2007.

[12] Ghoshal, A., and John, V. "A Method to Improve PLL Performance under Abnormal Condition, Thirty- Sixth IAS Annual Meeting." Conference Record of the 2011 IEEE Indian institute of science, vol.4, pp.2-6, 2011.

[13] Arruda L. N.; S. M. Silva, and B. J. C. Filho. "PLL structures for utility connected systems in IEEE Industry Applications Conference." Rec. 36th IEEE - IAS Annual Meeting, vol.4, pp.2655 –

2660, 2001.

[14] Ghoshal, A and Vinod, J. A Method To Improve PLL Performance Under Abnormal Grid Conditions. In: National Power Electronics Conference 2007. Indian Institute of Science, Bangalore, 2007.

[15] Padua, M. S. Frequency-Adjustable Positive Sequence Detector for Power Conditioning Applications, in 2005 IEEE 36th Power Electronics Specialists Conference, 36: pp.1928 – 1934, 2005.

[16] Glad, T and Ljung, L. Reglerteknik. GrundlΣggande Teori. Upplaga 4:4,Studentlitteratur, denmark, 2008.

[17] D. S. Henderson and D. E. Macpherson, "Application of solid state switching devices to electronic load governing of micro hydro generators," 1993 Fifth European Conference on Power Electronics and Applications, Brighton, UK, 1993, pp. 244-249 vol.8.

[18] D. Melly, R. Horta, C. Münch, H. Biner and S. Chevailler, "Development of a PM-generator for a counter-rotating micro-hydro turbine," 2014 International Conference on Electrical Machines (ICEM), Berlin, 2014, pp. 124-129.

[19] Krishna Kumar M J, Vinod John, "Comparison of 3-phase, 3-level UPF Rectifier Circuits for High Power Applications", IEEE International Conference on Power Electronics, Drives and Energy Systems, Bengaluru, India, 2012.

[20] K. T. Atta, A. Johansson, M. J. Cervantes and T. Gustafsson, "Maximum power point tracking for micro hydro power plants using extremum seeking control," 2015 IEEE Conference on Control Applications (CCA), Sydney, NSW, 2015, pp. 1874-1879.

[21] F. Blaabjerg, M. Liserre, and K. Ma, "Power electronics converters for wind turbine systems," IEEE Transactions on Industry Applications, vol. 48, no. 2, pp708-719, 2012

[22] A.L. Quilisch, *Object Oriented Modelling and Simulation of Kaplan Turbines,* Masters' Degree Project Stockholm, Sweden February 2008

[23] Abubeker Negesa Gemeda. "Design and Simulation of Cross Flow Turbine on Huluka River in Ethiopia," International Journal of Advance Engineering and Research Development, Vol. 5, PP. 1007-1017, March-2018.

[24] Kundur P., Neal J.B., and Mark G.L., "Power System Stability and Control", McGrawHill, 1994.

[25] K. Menny, Strömungsmaschinen – Hydraulische und thermische Kraft- und Arbeitsmaschinen, Verlag, Ronnenberg, Germany, 2006.

[26] Morimoto, S., Trend of permanent magnet synchronous machines. IEEJ Trans Elec Electron Eng, 2: 101 –108. doi:10.1002/tee.20116,2007.

[27] M. Singh, Adaptive Network-Based Fuzzy Inference Systems for Sensorless Control of PMSG Based Wind Turbine With Power Quality Improvement Features. (Doctoral dissertation). Retrieved from ProQuest Dissertation and Thesis.

[28] V. Bobek, PMSM Electrical Parameters Measurement. Free scale Semiconductor Application Note. Document Number:AN4680 Rev. 0, 02/2013

[29] Wind Resource: Utilising Hydrogen Buffering. (n.d.). Retrieved June 04, 2019, from http://www.esru.strath.ac.uk/EandE/Web_sites/08-09/Hydrogen_Buffering/Website%20Power%20Conditioning.html

[30] M.H. Rashid (ed.), *Power Electronics Handbook* (Academic Press, 2001).

[31] Step Up Boost Regulator or Converter. (n.d.). Retrieved June 04, 2019, from http://www.electronics-notes.com/articles/analogue circuits/power-supply-electronics/switching-step-up-boost-regulator-dc-dc-converter.php

[32] Mohan, N., .., M., Robbins, W. P., & Undeland, T. M. (1995). Power electronics: converters, applications, and design. New York, NY: Wiley.

[33] Bandana Bhutia, Dr. S.M.Ali, Narayan Tiadi. "Design of Three Phase PWM Voltage Source Inverter For Photovoltaic Application." International Journal of Innovative research in Electrical, Electronics, Instrumentation and Control Engineering, *Vol. 2, Issue 4, April 2014.*

[34] Milan Pradanovic& Timothy Green, Control and filter design of three phase inverter for high power quality grid connection, IEEE transactions on Power Electronics,Vol.18. pp.1 - 8, January 2003 .

[35] C Y Wang,Zhinhong Ye& G.Sinha, Output filter design for a grid connected three phase inverter,‖ Power electronics Specialist Conference, pp.779-784,PESE 2003

[36] Samul Araujo& Fernando Luiz, LCL fiter design for grid connected NPC inverters in offshore wind turbins,‖ 7th International conference on Power Electronics, pp. 1133-1138, October 2007.

[37] Kaura, V., and Blasko, V. Operation of a Phase Looked Loop System under Distorted utility conditions. IEEE Transactions on Industry Applications, vol.33, pp.58 - 63, 1997.

APPENDICES

Appendix A: MATLAB codes

PLL_koeff.m

```
%Calculating Kpll and Tpll using symmetrical optimum method
fbw = 50; %The Crossover frequency in Hz
ts = 1/2000;  %Sampling time
Vm = 380; %Amplitude of input sine waves
wc = 2*pi*fbw;
%Symmetrical optimum eq. (21)
a = 1/(wc*ts)
Ti = a^2*ts
Kp = (1/a)*(1/(Vm*ts))
```

Ideal_input_PLL.m

```
%Creates input signals for PLL used by the "To Workspace" box
%in SIMULINK
ts = 1/2000; %Sampling period
T = 0.2; %Simulating time
f = 50; %frequency in Hz
t = (0:ts:T)'; %Sampled time vector
Vm = 380; %Amplitude of the signals
%Balanced three phase signals
Va = Vm*sin(2*pi*f*(t+10*ts));
Vb = Vm*sin(2*pi*f*(t+10*ts - 1/(f*3)));
Vc = Vm*sin(2*pi*f*(t+10*ts + 1/(f*3)));
%Creates a reference signal with decreased amplitude
VaRef = (10/Vm)*Va;
simin = [t,Va,Vb,Vc,VaRef];
```

InputVarAmp_PLL.m

```
%Creates input signals with amplitude variation
ts = 1/2000; %Sampling period
T = 0.2; %Simulating time
f = 50; %frequency
Tp = 1/50; %period
Vm = 380; %Amplitude
t1 = (0:ts:2*Tp)';
t2 = (2*Tp+ts:ts:T)';
t = [t1;t2];
Va1 = Vm*sin(2*pi*f*(t1));
Va2 = 0.90*Vm*sin(2*pi*f*(t2)); %90 percent of Amplitude
Va = [Va1;Va2];
t1 = (0:ts:2*Tp+(1/(f*3)))';
t2 = (2*Tp+(1/(f*3)):ts:T)';
Vb1 = Vm*sin(2*pi*f*(t1- 1/(f*3)));
Vb2 = 0.90*Vm*sin(2*pi*f*(t2- 1/(f*3)));
Vb = [Vb1;Vb2];
t1 = (0:ts:2*Tp+(2/(f*3)))';
t2 = (2*Tp+(2/(f*3)):ts:T)';
Vc1 = Vm*sin(2*pi*f*(t1+ 1/(f*3)));
Vc2 = 0.90*Vm*sin(2*pi*f*(t2+ 1/(f*3)));
Vc = [Vc1;Vc2];
VaRef = (10/Vm)*Va;
simin = [t,Va,Vb,Vc,VaRef];
x = [2*Tp + 10*ts, T];
h = [0.91*Vm, 0.91*Vm];
figure
plot(x,h, 'k--' )
hold on
plot(t, Va)
```

```
plot(t, Vb, 'r' )
plot(t, Vc, 'g' )
legend( '90% of amplitude' )
```

Input Phase Jump.m

```
%Creates input signals with a phase jump
ts = 1/2000; %Sampling period
T = 0.2; %Simulating time
f = 50; %frequency
Tp = 1/50; %period
Vm = 380; %Amplitude
t1 = (0:ts:4*Tp+11*ts)';
t2 = (4*Tp+(11+15)*ts:ts: T+14*ts)';
t = (0:ts:T)';
Va1 = Vm*sin(2*pi*f*(t1));
Va2 = Vm*sin(2*pi*f*(t2));
Va = [Va1;Va2];
Vb1 = Vm*sin(2*pi*f*(t1- 1/(f*3)));
Vb2 = Vm*sin(2*pi*f*(t2- 1/(f*3)));
Vb = [Vb1;Vb2];
Vc1 = Vm*sin(2*pi*f*(t1+ 1/(f*3)));
Vc2 = Vm*sin(2*pi*f*(t2+ 1/(f*3)));
Vc = [Vc1;Vc2];
VaRef = (10/Vm)*Va;
simin = [t,Va,Vb,Vc,VaRef];
figure
plot(t, Va)
hold on
plot(t, Vb, 'r' )
plot(t, Vc, 'g' )
```

AmpUnbalance_PLL.m

```
%Creates input signals with unbalanced amplitudes
%for PLL used by the "To Workspace" box in SIMULINK
ts = 1/2000; %Sampling period
T = 0.2; %Simulating time
f = 50; %frequency in Hz
t = (0:ts:T)'; %Sampled time vector
Vm = 380; %Amplitude of the signals
%Voltage unbalanced three phase signals
Va = Vm*sin(2*pi*f*(t+10*ts));
Vb = 0.85*Vm*sin(2*pi*f*(t+10*ts - 1/(f*3))); %15 percent decreased ampl
Vc = 1.15*Vm*sin(2*pi*f*(t+10*ts + 1/(f*3))); %15 percent increased ampl
%Creates a reference signal with decreased amplitude
VaRef = (10/Vm)*Va;
simin = [t,Va,Vb,Vc,VaRef];
close all
plot(t, Va)
hold on
plot(t, Vb, 'r' )
plot(t, Vc, 'g' )
title( 'Input signals with unbalanced amplitudes' )
xlabel( 'Time [s]' )
ylabel( 'Voltage [V]' )
legend( 'Va' , 'Vb' , 'Vc' )
axis([0, 2*(1/f), -1.2*Vm, 1.2*Vm]);
```

Improper Phase Shift_PLL.m

```
%Creates input signals with phase shift different from 120 degree
%for PLL used by the "To Workspace" box in SIMULINK
ts = 1/2000; %Sampling period
T = 0.2; %Simulating time
```

```
f = 50; %frequency in Hz
t = (0:ts:T)'; %Sampled time vector
Vm = 380; %Amplitude of the signals
%Balanced three phase signals
Va = Vm*sin(2*pi*f*(t+10*ts));
Vb = Vm*sin(2*pi*f*(t+10*ts - 1/(f*3) - 1/(36*f))); %10 percent decreased ampl
Vc = Vm*sin(2*pi*f*(t+10*ts + 1/(f*3) + 1/(36*f))); %10 percent increased ampl
%Creates a reference signal with decreased amplitude
VaRef = (10/Vm)*Va;
simin = [t,Va,Vb,Vc,VaRef];
close all
plot(t, Va)
hold on
plot(t, Vb, 'r' )
plot(t, Vc, 'g' )
title( 'Input signals with improper phase shifts' )
xlabel( 'Time [s]' )
ylabel( 'Voltage [V]' )
legend( 'Va' , 'Vb' , 'Vc' )
axis([0, 2*(1/f), -1.15*Vm, 1.15*Vm]);
```